0004893

FAA-RD-71-99

EXPERIMENTAL ATMOSPHERIC ABSORPTION COEFFICIENTS

Carole S. Tanner

EG&G

HYDROSPACE RESEARCH CORPORATION
1360 Rosecrans Street
San Diego, California 92106

transpo 72
U.S. International Transportation Exposition
Dulles International Airport
Washington, D.C.
May 27-June 4, 1972

NOVEMBER 1971

FINAL REPORT

Availability is unlimited. Document may be released to the National Technical Information Service, Springfield, Virginia 22151, for sale to the public.

DEPARTMENT OF TRANSPORTATION
FEDERAL AVIATION ADMINISTRATION
Systems Research and Development Service
Washington, D.C. 20591

The contents of this report reflect the views of the Hydrospace Research Corporation, which is responsible for the facts and the accuracy of the data presented herein. The contents do not necessarily reflect the official views or policy of the Department of Transportation. This report does not constitute a standard, specification, or regulation.

TECHNICAL REPORT STANDARD TITLE PAGE

1. Report No. FAA-RD-71-99	2. Government Accession No.	3. Recipient's Catalog No.
4. Title and Subtitle EXPERIMENTAL ATMOSPHERIC ABSORPTION COEFFICIENTS		5. Report Date NOVEMBER 1971
		6. Performing Organization Code
7. Author(s) Carole S. Tanner		8. Performing Organization Report No.
9. Performing Organization Name and Address Hydrospace Research Corporation 1360 Rosecrans Street San Diego, California 92106		10. Work Unit No. 550-002-07H
		11. Contract or Grant No. DOT FA70WA-2374
12. Sponsoring Agency Name and Address Federal Aviation Administration Systems Research and Development Service 800 Independence Avenue, S.W. Washington, D.C. 20591		13. Type of Report and Period Covered Final Report June 1970-November 1971
		14. Sponsoring Agency Code
15. Supplementary Notes		

16. Abstract

The objective of this work was to acquire experimental data on atmospheric sound absorption and sideline noise propagation for the purpose of updating and refining aircraft noise measurement standards and improving aircraft noise prediction techniques. The effort involved acquisition of acoustical, meteorological, aircraft tracking, and aircraft operational data. The sound source was a Lockheed T-33A aircraft, propelled by a single Allison J33-A-35 turbojet engine, operating at constant thrust in level flight. Microphones were located near the ground in an array normal to the flight track. All tests were conducted at the Pendleton Municipal Airport, Pendleton, Oregon during two separate time periods in July and September 1970.

17. Key Words Acoustics Atmospheric Sound Absorption Sideline Noise Propagation	18. Distribution Statement Availability is unlimited. Document may be released to the Clearinghouse for Federal Scientific and Technical Information, Springfield, Virginia 22151 for sale to the public.

19. Security Classif. (of this report) UNCLASSIFIED	20. Security Classif. (of this page) UNCLASSIFIED	21. No. of Pages	22. Price $3/pc $.95/mc

Form DOT F 1700.7 (8-69)

TABLE OF CONTENTS

	Page
INTRODUCTION	1
APPARATUS AND METHODS	5
Test Aircraft	5
Tracking Data	5
Meteorological Data	9
Acoustic Data	11
Data Analysis	19
Aircraft	19
Weather	19
Acoustic Data	31
CONCLUSIONS	57
REFERENCES	59
APPENDIX A - FLYBY MEASUREMENT GEOMETRY	A-1

LIST OF ILLUSTRATIONS

Figure		Page
1	Topographical Features of Test Area	7
2	Radar Tracking Unit	8
3	Phototheodolite Unit	9
4	Weather Aircraft	10
5	Sounding Profile	11
6	Typical Microphone Site	12
7	System Frequency Response	13
8	San Diego Computer Facility	14
9	Analysis Concept	15
10	Elevation Angle as a Function of Slant Range for Values of Aircraft Height and Microphone Position	17
11	Aircraft Weather Sounding	20
12	Radiosonde Weather Sounding	25
13	Surface Weather Measurements	29
14	Atmospheric Absorption Coefficients for One-Third Octave Bands of Noise for Different Temperatures and Humidities	32
15	Variation of Spectra, 1500-Foot Flyby	33
16	Variation of Spectra, 100-Foot Flyby	34
17	Variation of Spectra at Site 1 as a Function of Test Altitude	35
18	Variation of Spectra at Site 2 as a Function of Test Altitude	35
19	Sound Absorption Coefficients, Test Group 1	38
20	Sound Absorption Coefficients, Test Group 2	40
21	Sound Absorption Coefficients, Test Group 3	42
22	Sound Absorption Coefficients, Test Group 4	44

LIST OF ILLUSTRATIONS (Contd)

Figure		Page
23	Sound Absorption Coefficients, Test Group 5	46
24	Sound Absorption Coefficients, Test Group 6	48
25	Sound Absorption Coefficients, Test Group 7	50
26	Sound Absorption Coefficients, Test Group 8	52
27	Sound Absorption Coefficients, Test Group 9	54
28	Sound Absorption Coefficients, Test Group 10	55

LIST OF TABLES

Table		Page
I	Aircraft and Engine Specifications	6
II	Average Aircraft Parameters	8
III	Meteorological Parameters	9
IV	Optimum Radiation Angles	16

LIST OF SYMBOLS

d_A	Distance from microphone to sound source for position A – feet
d_B	Distance from microphone to sound source for position B – feet
SPL_A	Normalized sound pressure level at position A – dB
SPL_B	Normalized sound pressure level at position B – dB
X	Distance along perpendicular to runway centerline – feet
Y	Distance along runway centerline – feet
Z	Height above reference point – feet
α	Atmospheric absorption coefficient
β	Angle of slant range with respect to the ground – degrees
θ	Sound source directivity angle measured from the front end of the aircraft

INTRODUCTION

The basic objective of this project was to elicit experimental data on atmospheric sound absorption and sideline noise propagation for the purpose of constructing aircraft noise measurement standards and improving noise prediction techniques.

To ensure a significant measure of improvement and consistency over previous experiments, emphasis was placed on the following factors:

(1) Three-dimensional monitoring of atmospheric conditions in the area of sound propagation by means of surface, balloon, and aircraft meteorological instrumentation.

(2) Careful choice of an airborne sound source and acoustic measurement instrumentation to minimize difficulty in extracting sound attenuation values as a function of frequency.

(3) Careful attention to the flight program in monitoring of aircraft position, engine operation, flight direction, and test run sequence.

(4) Analysis of acoustic data and correlation of acoustic weather data to minimize the influence of sound propagation factors other than those sought for in the measured data.

The secondary objective of this project was to develop an acoustic data bank consisting of effective perceived noise levels (EPNL) versus slant range (SR) for military as well as civil aircraft. These data which serve to expand noise exposure forecasting capabilities are reported in Reference 1.

The basic program approach involved four specific types of data: acoustic, meteorological, tracking, and aircraft data. The program was conducted in two phases with test periods in July and September 1970.

All tests were conducted at the Pendleton Municipal Airport, Pendleton, Oregon. This site was chosen because it met a majority of the following requirements:

(1) Low aircraft traffic

(2) Good topography

(3) Meteorological facilities

(4) Instrumented runway

(5) Low noise background

(6) Land availability for microphone placement

(7) Favorable atmospheric conditions

The map in Figure 1 illustrates the main topographical features of the test area. The ground is gently rolling and was planted in wheat or lying fallow. The majority of the area over which sound propagated was fallow. The soil is composed of silt and was cultivated to yield a rather rough textured surface.

Climatologically, the test area is located in the southeastern part of the Columbia Basin and is a semiarid area. The local weather conditions encountered during the two test periods varied from extremely hot days (95-100°F) in July to moderate temperatures (40-50°F) in September. Precipitation did occur during the September test period.

The microphone locations for noise measurements are shown in Figure 1. These locations and their elevations were marked during a survey. Noise measurements were made by eight microphones placed in pairs. One microphone was located near the ground and the other microphone mounted at a height of 26 feet, directly above the ground microphone. Original plans called for mounting the ground microphone flush with the surface, however, the dusty environment precluded this step.

The July tests used microphones located 500, 1000, 1500, and 2000 feet from the runway centerline. This was subsequently altered to 250, 500, 1000, and 1500 feet for the September tests.

As stated previously, the program was conducted in two phases. The basic test plane of Phase 1 included the steps discussed below and was subsequently modified for Phase 2.

The test aircraft, a T-33A, flew a series of two level flybys at altitudes of 2000, 1500, 700, and 100 feet above the runway centerline. The level flight was maintained over the length of the test site as shown by the outline in Figure 1. Each altitude was repeated once, therefore, a test series or group consists of eight runs. The test aircraft was tracked using both a tracking radar and a phototheodolite system. Immediately after the T-33A had made its pass, an instrumented weather aircraft made a weather sounding.

During the course of the test periods, weather data from the ESSA weather station and radiosonde balloon data were obtained.

Based on the test experience during July, a number of improvements and changes to the test plan were made for the September tests. The basic areas of improvement were as follows:

(1) Reinstrumenting the weather aircraft

(2) Providing additional surface weather measurements

(3) Modifying the sounding profile

(4) Moving the microphone array closer to the runway

Due to these improvements, this report will present only details of the instrumentation and data used during the Phase 2 September tests.

The report will describe the details of data acquisition and data reduction of 1) aircraft data, 2) tracking data, 3) weather data, and 4) acoustic data. Detailed weather data are shown and comparisons of test data and current atmospheric absorption coefficients are included.

APPARATUS AND METHODS

TEST AIRCRAFT

The test aircraft, a Lockheed T-33A, registration number 156, flew eight straight and level flybys during a test period. These eight runs were performed, in general, within a time period of one hour.

The T-33A is a single engine turbojet aircraft. Aircraft and engine specifications are given in Table I. Aircraft performance was noted on a flight test card. Typical average parameters experienced during the entire test are given in Table II. The engine power was kept at a nominal 100 percent and the pilot endeavored to maintain an indicated airspeed of approximately 165 knots. As the aircraft gross weight decreased during a set of runs, the use of speed brakes and flaps were employed to offset increases in speed.

TRACKING DATA

The test aircraft was tracked using both a radar and phototheodolite system. These two tracking systems were located as shown in Figure 1.

The radar unit, a portable MPS-19 system, is shown in Figure 2. The unit both records on tape and plots out X, Y, and Z coordinate information. Since the test aircraft was not instrumented with a beacon, the aided tracking mode was utilized. This mode of operation utilizes visual tracking of the aircraft with the aid of a long-range television camera. Azimuth and elevation are obtained from the optical system and range obtained using skin tracking. The aircraft wing root was the selected tracking point.

The phototheodolite units consisted of two Ackley cameras located as shown in Figure 1. The instrument, shown in Figure 3, is an optical tracking unit having a movie camera triggered electronically at the rate of two frames per second. The film field of view included the aircraft and the azimuth and elevation dials. The location of the theodolites perpendicular to the runway requires the assumption that the aircraft is flying down the runway centerline. The output is Y, Z, and velocity as a function of time.

Both the radar and phototheodolite data were reduced to the appropriate coordinate values. In this report, X coordinate is crossrange, Y coordinate is downrange, and Z coordinate is height above the reference point. The

Table I. Aircraft and Engine Specifications

T-33A AIRCRAFT

Specifications:	Span	38 ft 10-1/2 in.
	Length	37 ft 9 in.
	Height	11 ft 4 in.
	Weight - empty	8084 lb
	- loaded	11,965 lb
	Power plant	J33-A-35

Performance:

Maximum speed at sea level	600 mph
at 25,000 ft	543 mph
Stalling speed (with flaps)	102 mph
(without flaps)	113 mph
Climb to 25,000 ft	6.5 min
Service ceiling	47,500 ft
Landing distance from 50 ft alt	3480 ft
Endurance	3.12 hr

J33-A-35 - TURBOJET ENGINE

Description:

a. Single stage centrifugal compressor (4.4:1 pressure ratio, 86 pps airflow.

b. 14 straight-through combustors.

c. Single-stage turbine (T.I.T. = 1550°F, T.E.T. = 1265°F at 11,750 rpm).

Specifications:	Diameter	49.2 in.
	Length	104.5 in.
	Weight	1795 lb
	Thrust	5200 lb (dry) - takeoff
		3900 lb - maximum continuous

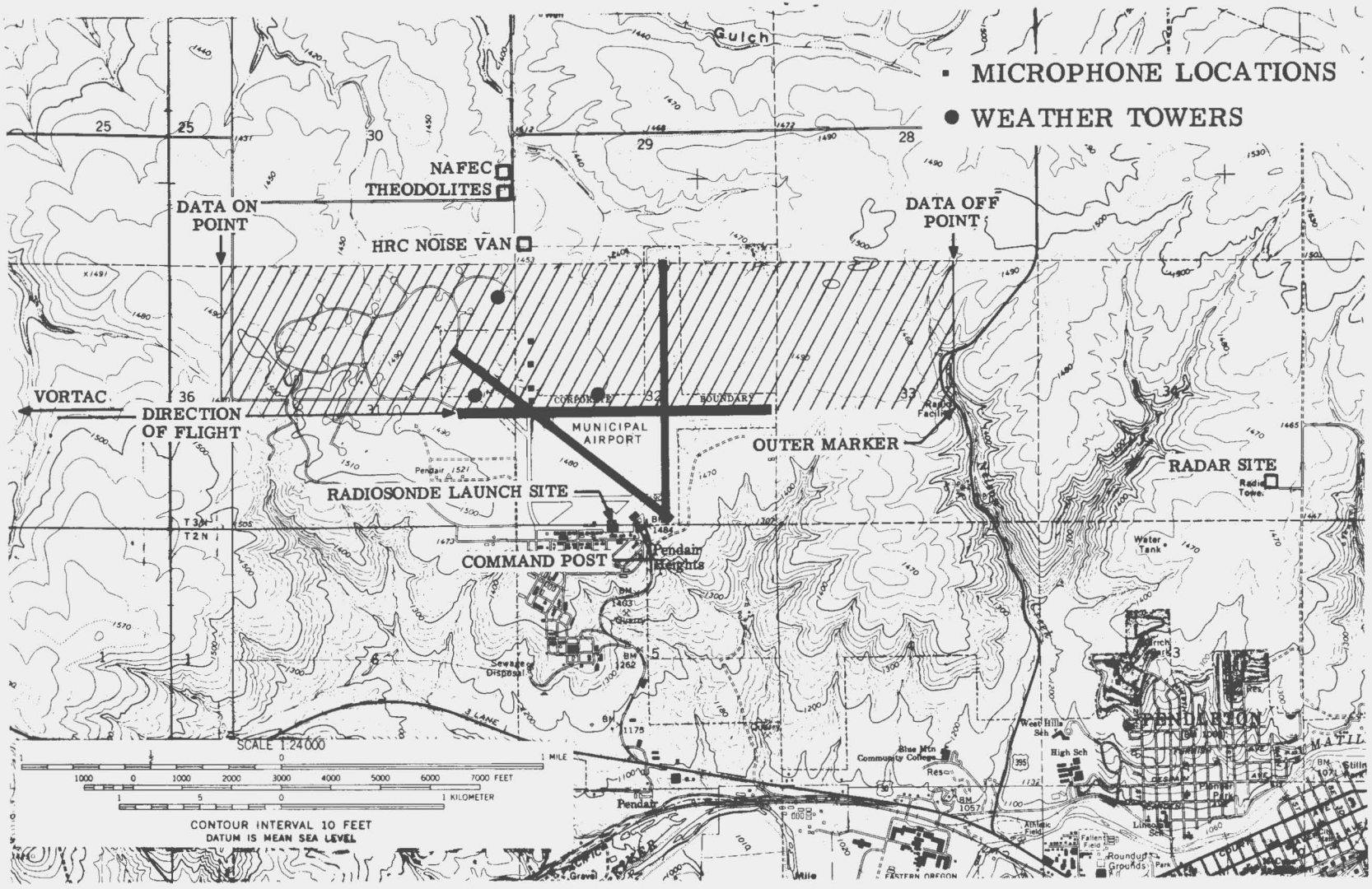

Figure 1. Topographical Features of Test Area

Table II. Average Aircraft Parameters

Flight No.	Aircraft Weight (lb)	Indicated Airspeed (kt)
1	14,260 ±200	162 ±3
2	13,800 ±200	161 ±3
3	13,310 ±200	162 ±3
4	12,840 ±200	163 ±3
5	12,390 ±200	165 ±3
6	11,980 ±200	166 ±3
7	11,490 ±200	167 ±3
8	10,870 ±200	168 ±3

Figure 2. Radar Tracking Unit

Figure 3. Phototheodolite Unit

reference point for all tracking data was chosen as the intersection of the runway centerline and a line passing through the microphone positions.

The tracking data were output both as hard copy and recorded on digital magnetic tape. These tapes were later used to calculate the slant range and the time of arrival of sound at a specified radiation angle.

METEOROLOGICAL DATA

The meteorological parameters acquired are summarized in Table III. Three types of weather observations were made: 1) surface, 2) radiosonde, and 3) aircraft soundings.

The surface observations consisted of data acquired at three towers located as shown in Figure 1. In addition, wind velocity and direction were acquired at each

Table III. Meteorological Parameters

Type	Temperature	Relative Humidity	Wind Velocity	Wind Direction	Elevation (ft)	Frequency of Measurement
Aircraft	X	X			50 - 2500	Before every run
Radiosonde	X	X	X	X	0 - 3000	Bi-hourly
Surface T-1	X	X	X	X	6	Continuously
Surface T-1	X	X	X		50	Continuously
Surface T-2	X	X	X		50	Continuously
Surface T-3	X	X	X		50	Continuously
Surface T-1	X	X	X	X	100	Continuously
Surface			X	X	26	Every run
Surface	X	X	X	X	10	Hourly

microphone location. The instrumentation used consisted of standard wind direction and speed indicators and a thermistor and dew point temperature indicator.

Surface weather was recorded on strip charts during the entire test period. Data were extracted from these charts at the time of day associated with the closest point of approach of the aircraft to the line of microphones. The data were averaged over two minutes.

Radiosonde balloons were launched periodically during the test day. In general, these soundings provided data representative of each particular test period. The balloon was launched to the south of the test site at the location shown in Figure 1. The transponder was tracked via radio theodolite. The radiosonde yielded temperature and dew point averaged over a period of approximately 6 seconds. The weather tracking output occurred at 6-second intervals. Winds aloft were calculated from changes in balloon position, from one tracking point to the next.

Upper air soundings were also made using the aircraft shown in Figure 4. This aircraft flew a sounding profile shown in Figure 5. Meteorological instrumentation included a Cambridge Systems Model 137-C3/137-S3P hygrometer.

Figure 4. Weather Aircraft

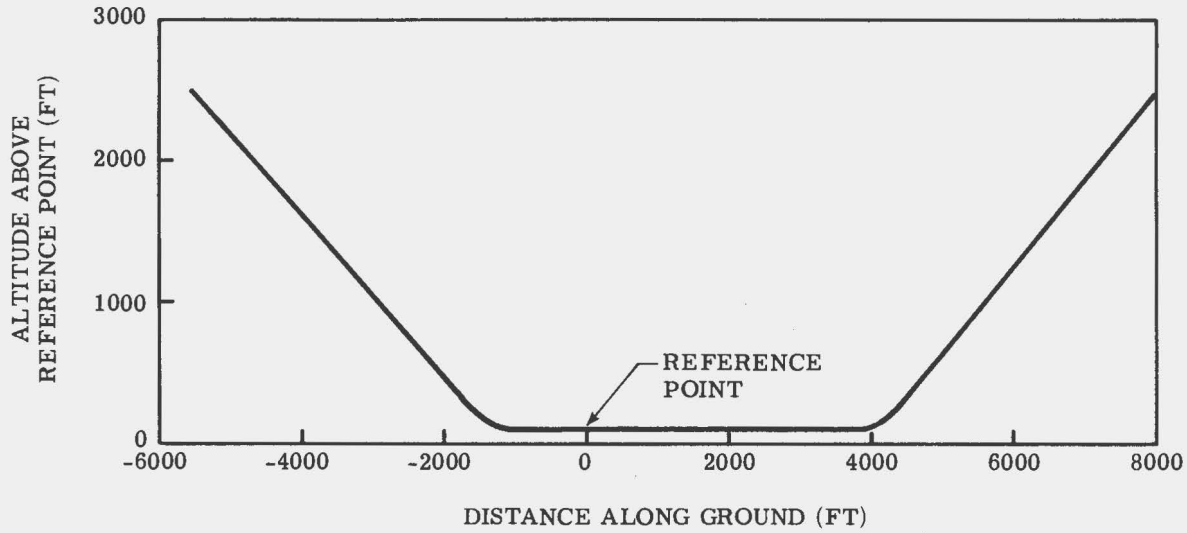

Figure 5. Sounding Profile

ACOUSTIC DATA

Acoustic data were acquired using eight microphone stations. A typical station, shown in Figure 6, consisted of a B&K 4134/2619 microphone-preamplifier and a 141A portable field unit. In addition, a Taylor anemometer and wind direction indicator were placed at the 26-foot level. Acoustic data was transmitted to the recording van using twisted shield pair cable terminated by a pair of transformers. The wind information was transmitted via a "phantom circuit."

Microphone data, voice, IRIG B time code, CPA tone mark, and wind information were recorded on 14-track analog tape in the acoustics van. The van contained communications gear, WWV receiver, and the Hydrospace Model 1360 portable field system. The latter includes IRIG time code, tape recorder, signal conditioning, and data processing equipment such as one-third octave band filters and a computer.

The microphone systems were calibrated using both an electrostatic actuator and an rms voltage input to the preamplifier over a frequency range of 12 Hz to 10,000 Hz. Typical total system response is shown in Figure 7. Note that pre-emphasis of approximately 6 dB/octave, starting at 1000 Hz, was used. Overall system dynamic range was 60 dB.

The microphone equipment was also calibrated for sound pressure level using an input of 94 dB at 1000 Hz. This calibration was performed before and after each test period.

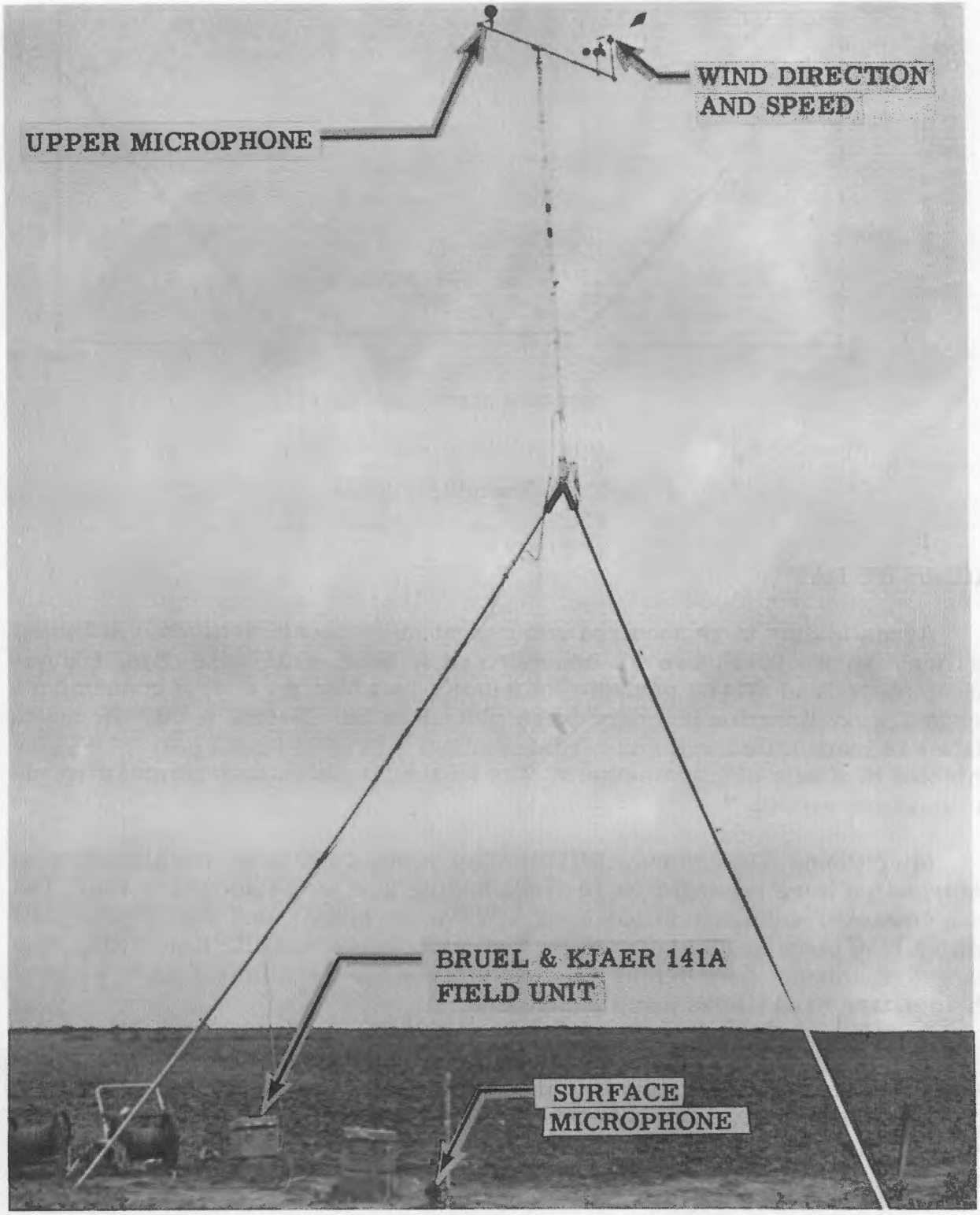

Figure 6. Typical Microphone Site

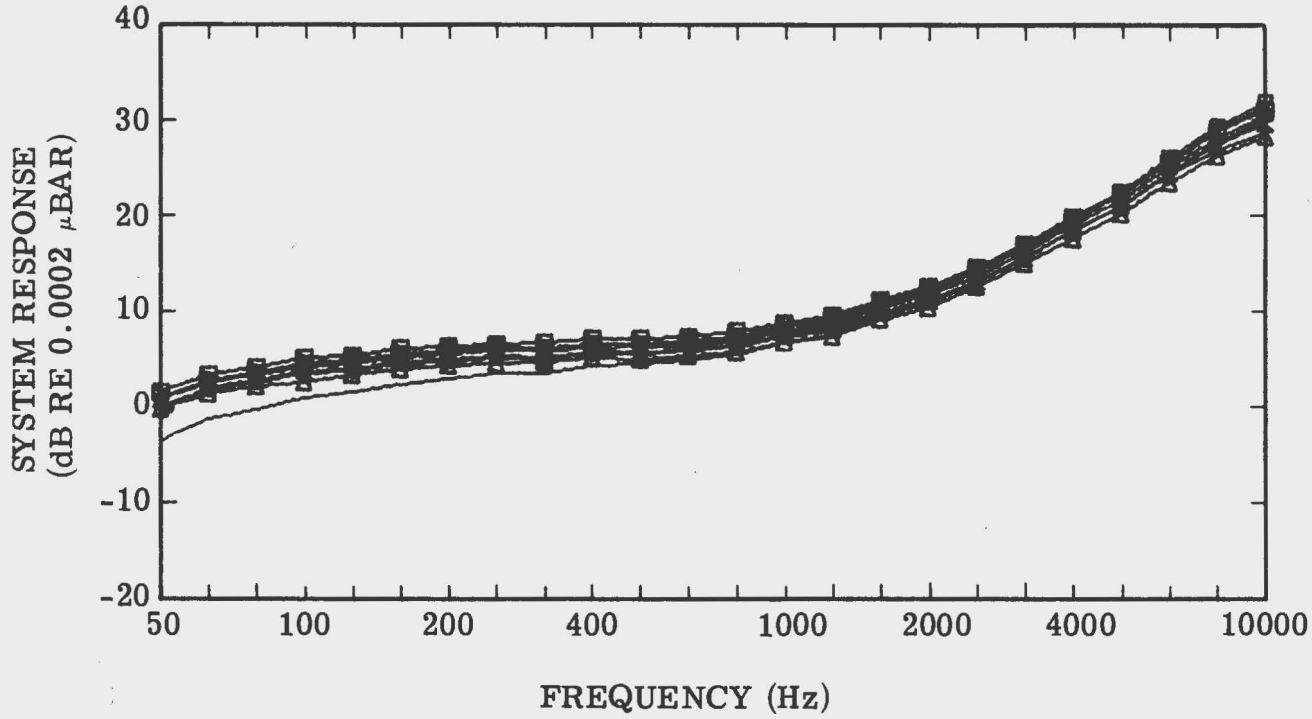

Figure 7. System Frequency Response

Since several independent groups were acquiring data, a standard range time based on WWV time, broadcast from Fort Collins, Colorado was used.

All timing systems were synchronized to this signal, thus assuring data correlation between tracking and acoustic data.

The time of closest point of approach (CPA) of the aircraft to the line of microphones was acquired as a back-up parameter in the event that the tracking systems became inoperable. The method used consisted of locating an observer at a distance of 2500 feet from the runway and in line with the microphones. The observer sighted down two guide poles and triggered a pushbutton which generated a tone signal to be recorded on tape. In addition, the signal generated an interrupt command to the computer which then read the time code and printed out the time of day on the teletype.

The acoustic data were processed using the system shown in Figure 8. The basic processing program acquired 60 one-half second spectra, starting at 4 seconds before CPA. This time period was sufficient to acquire the data of interest. The final spectra are stored on digital tape, along with the necessary descriptors of run, microphone number, and time.

Figure 8. San Diego Computer Facility

The analysis concept used is illustrated in Figure 9, which shows a simplified sketch of the aircraft flight path and the measurement positions. The correlation of the acoustical data will consist of comparing sound data as a function of range for the same angle of radiation, θ, from each of the microphones.

Using time correlations, the signal received at any instant of time at each microphone position can be related to the aircraft position, taking into account the average speed of sound.

This analysis makes the assumption that the aircraft noise output for any one flyover at constant airspeed and altitude is constant during the flyover. It further assumes axially symmetric sound radiation about the flight path and

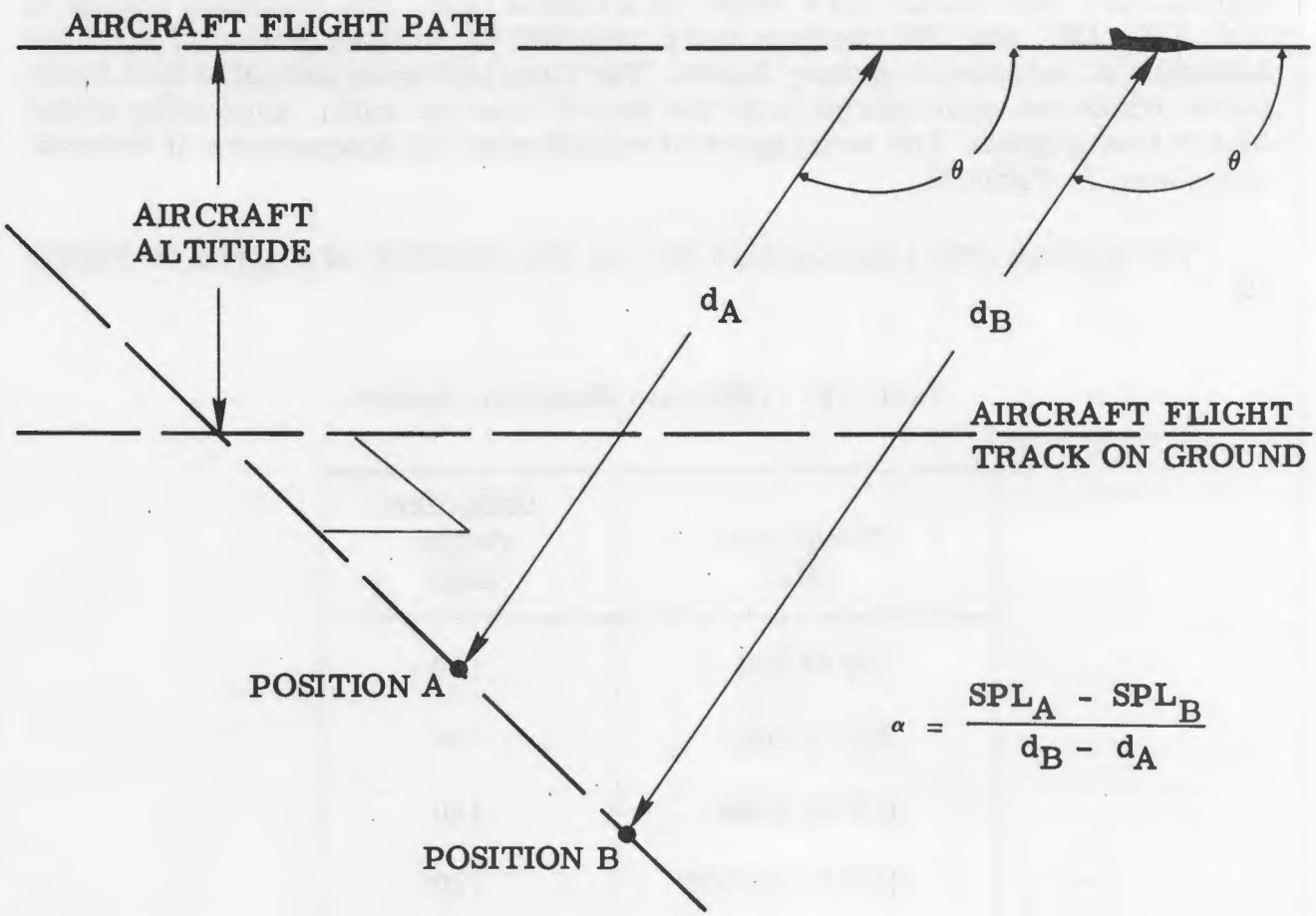

Figure 9. Analysis Concept

that the sound source is uniform from flight to flight. Since the aircraft has only one engine whose exhaust is located at the rear of the aircraft, it is assumed that the sound power output and directivity are uniform for flights made at different altitudes.

The sound digital tapes and radar digital tapes were merged utilizing a computer program. The program used preselected radiation angles of 110, 120, 130, and 140 degrees as inputs to compute the cosine of the angle between the flight path and the slant range to the microphones for each X, Y, Z, and time radar input. The program selected the time at which $\theta_{calc} = \theta_{input}$, within 0.5 seconds, and using the average speed of sound calculated the time of arrival of the sound at each microphone location. The slant range at time of emission was also calculated. The time of arrival was used to search the acoustic digital tape and retrieve the proper spectrum. Details of the equation used are given in Appendix A. The spectrum was normalized to a distance of 500 feet using the inverse square law. The normalized spectrum and appropriate slant range were output on a digital tape. The radiation angles of 110, 120, 130, and 140 degrees were selected by an examination of the time histories of selected frequency bands. The time histories indicated that there were problems encountered with the signal to noise ratio, especially at the higher frequencies. The best angles of radiation for all frequencies of interest are shown in Table IV.

The geometrical relationships for all microphones are given in Figure 10.

Table IV. Optimum Radiation Angles

Frequency (Hz)	Radiation Angle (deg)
50 to 200	140
250 to 500	130
630 to 1000	120
1250 to 10,000	110

(a)

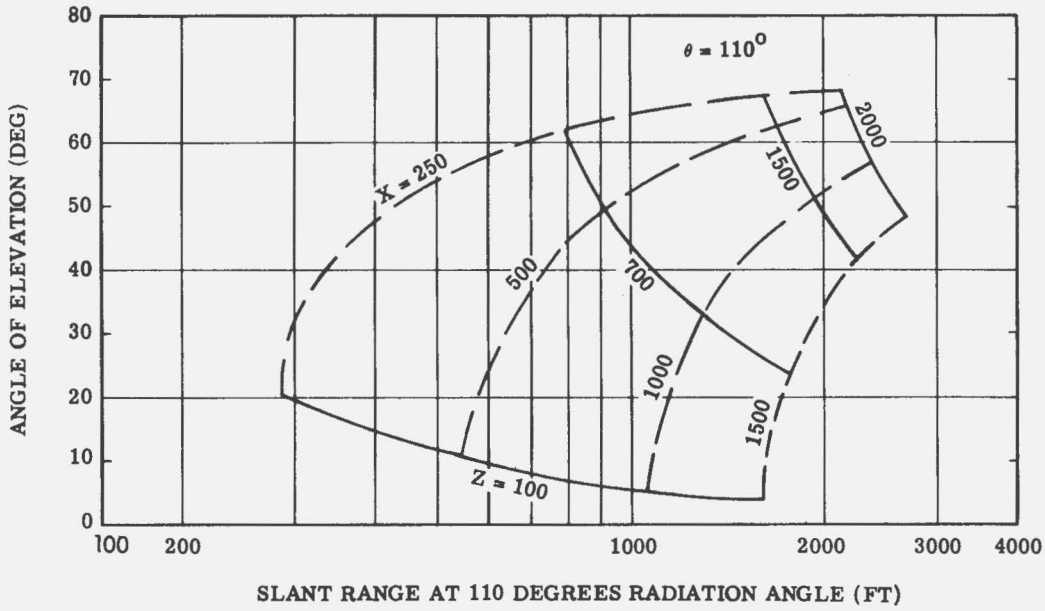

Radiation Angle (θ) = 110 Degrees

(b)

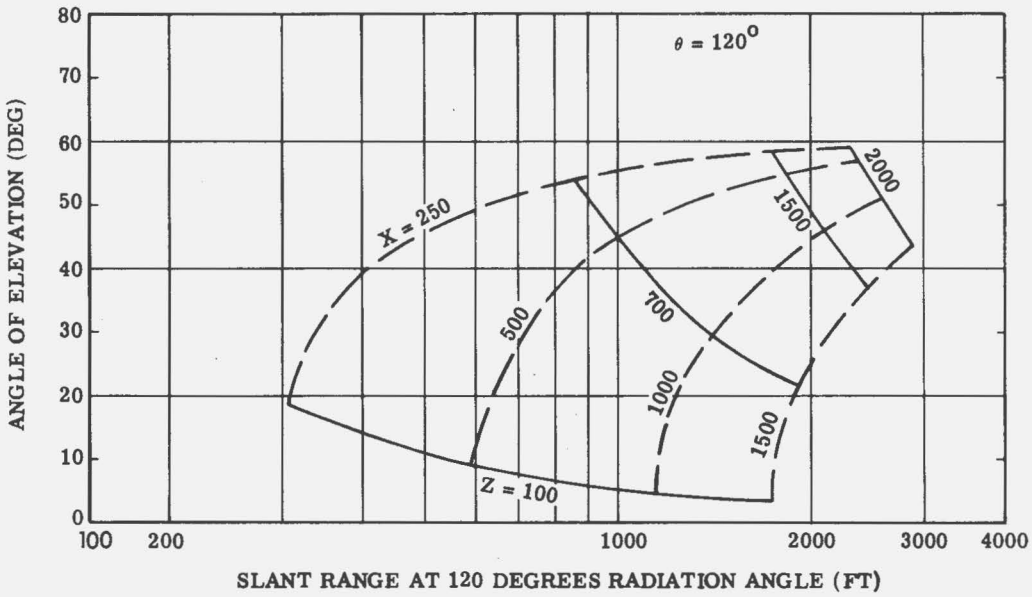

Radiation Angle (θ) = 120 Degrees

Figure 10. Elevation Angle as a Function of Slant Range for Values of Aircraft Height and Microphone Position

(c)

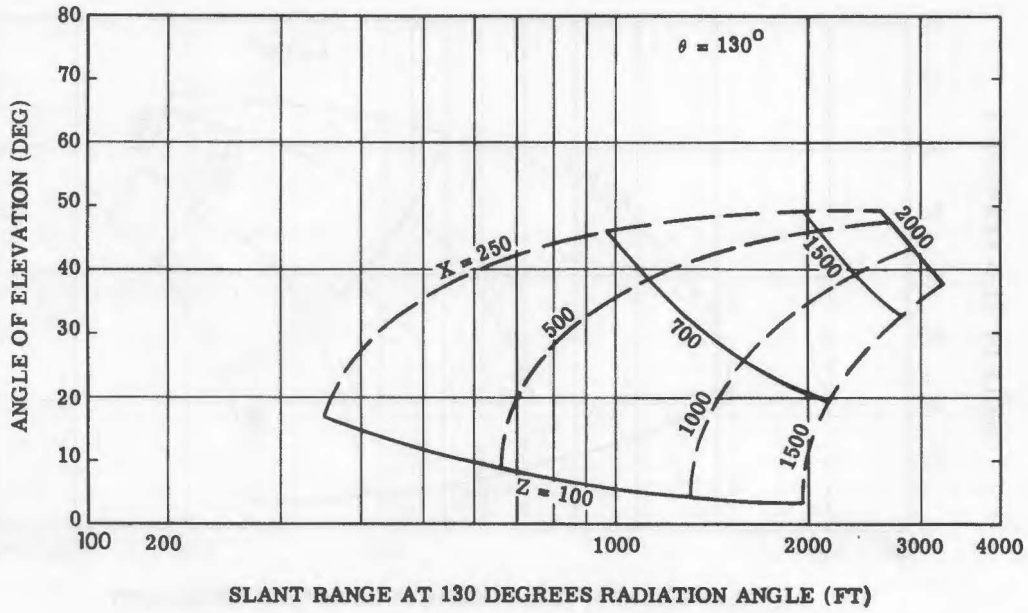

Radiation Angle (θ) = 130 Degrees

(d)

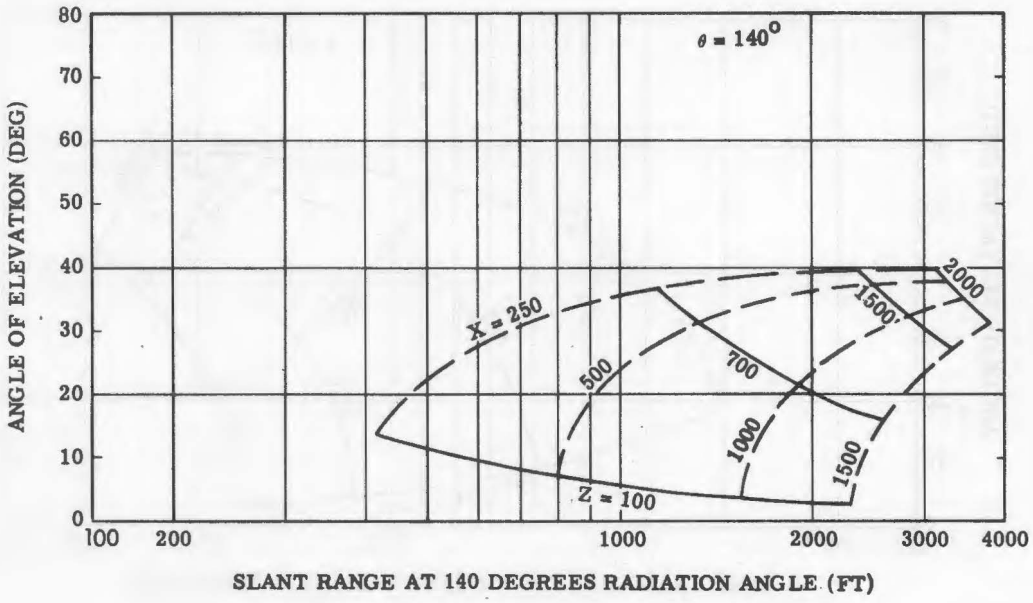

Radiation Angle (θ) = 140 Degrees

Figure 10. Elevation Angle as a Function of Slant Range for Values of Aircraft Height and Microphone Position (Contd)

DATA ANALYSIS

Aircraft

The data obtained from the test aircraft is shown in summary in Table II. The values were obtained by averaging the flight card data from each flyby and grouping according to altitude. Since the power was kept at a constant 100 percent, the sound pressure level could vary according to reductions in engine power as a function of altitude and outside air temperature and variations in jet relative velocity resulting from changes in airspeed. Using the estimation procedure in Reference 2, a 10-percent change in airspeed results in a 0.5-dB change of estimated sound level. Likewise, 10-percent change in thrust results in a 0.5-dB change in sound level. It is reasonable to assume that actual variations during the test were within these limits. Additional noise data for the T-33A is presented in Reference 1.

Since the test aircraft had a turbojet power plant, there was very little front end noise to complicate the identification of sources. The location of the exhaust at the rear of and on the centerline of the airplane also simplified source identification. Although the choice of the aircraft used did simplify the analysis, problems were encountered in obtaining sufficient high frequency noise at the larger slant ranges.

Weather

Meteorological data from the various sources are presented in ten groups, each group representing a test period. Data are presented to show the variation of parameters for the soundings, both aircraft and radiosonde. Also presented are the variations of values obtained from the surface measurements.

Figure 11 shows the variation in temperature, relative humidity, and absolute humidity, as a function of altitude above the reference point. These data are a composite of eight aircraft soundings per group.

Figure 12 shows changes in wind velocity and direction as a function of altitude for radiosonde soundings. With one exception, there were no repeats of radiosonde soundings within a test period. There were no radiosondes launched during the test period of groups 1 and 3.

The results of the surface measurements are shown in Figure 13 for all available parameters. These include measurements at the three tower locations and the microphone sites in the case of wind velocity. A comparison of the surface data gives some estimation of the uniformity of the weather over an area shaped somewhat like a triangle.

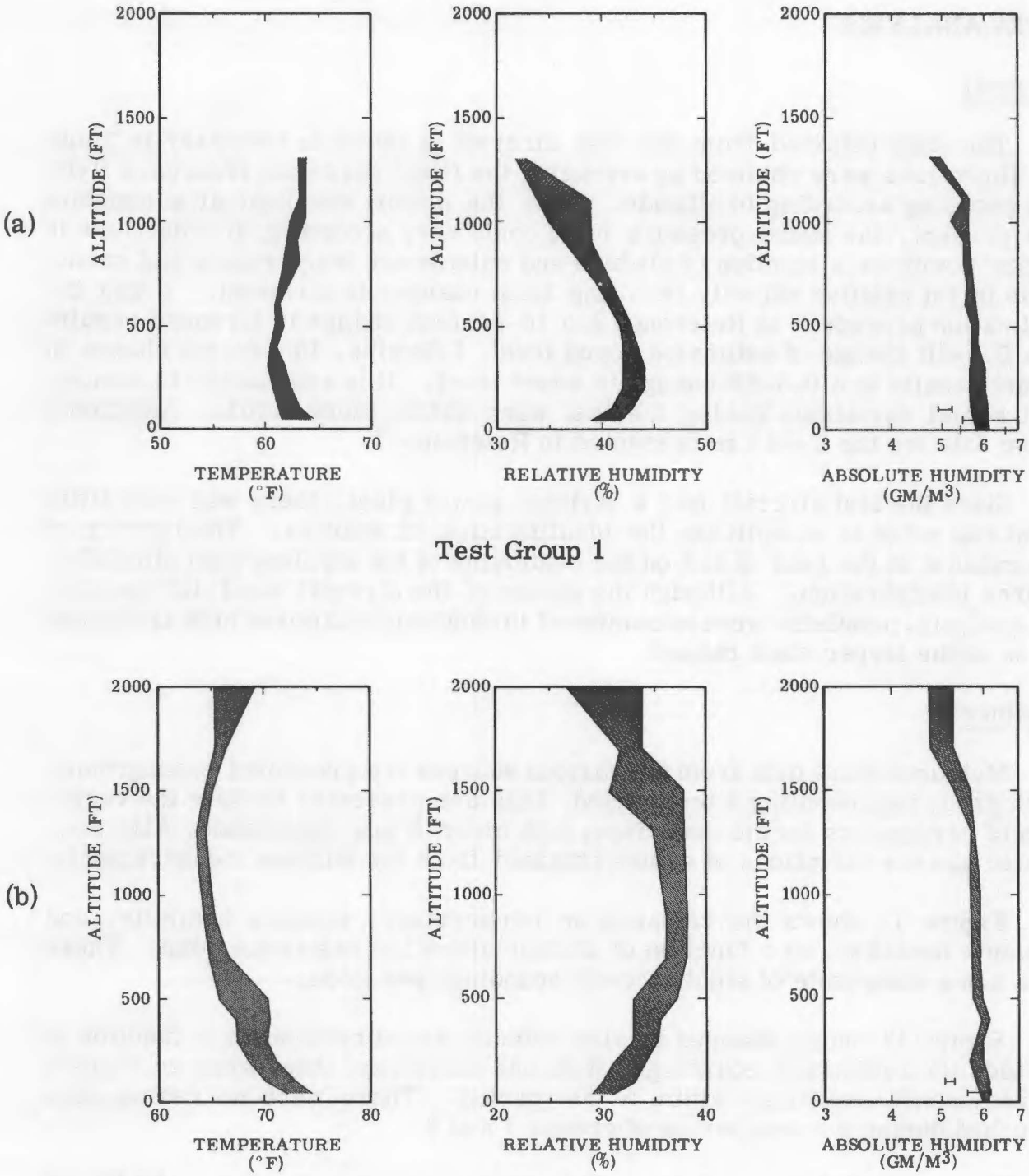

Figure 11. Aircraft Weather Sounding

(c)

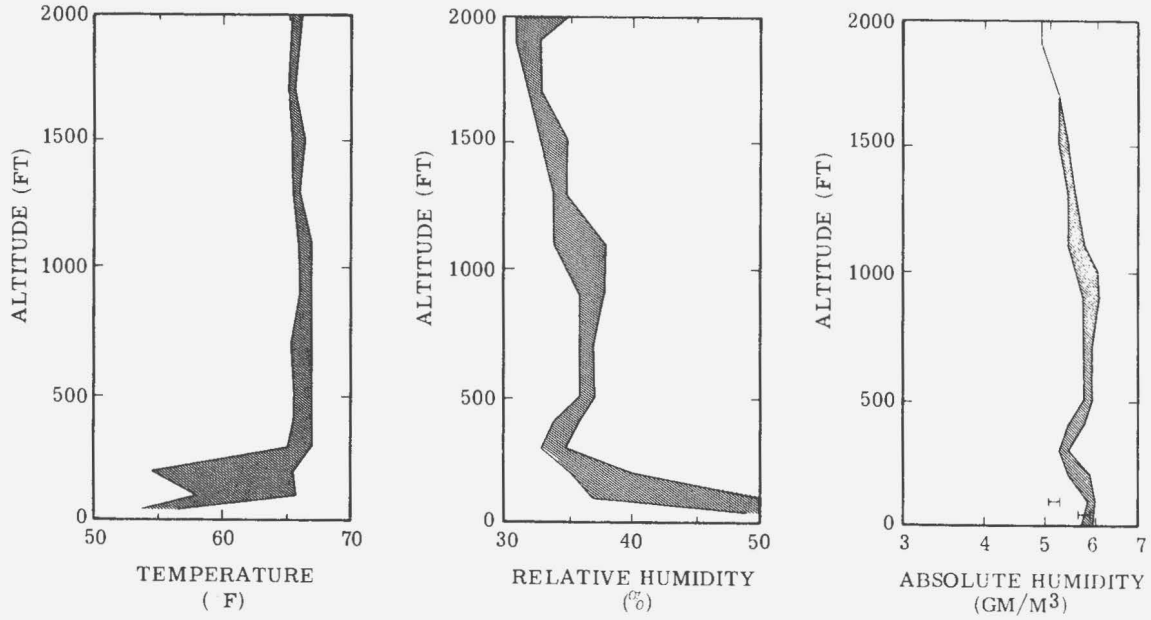

Test Group 3

(d)

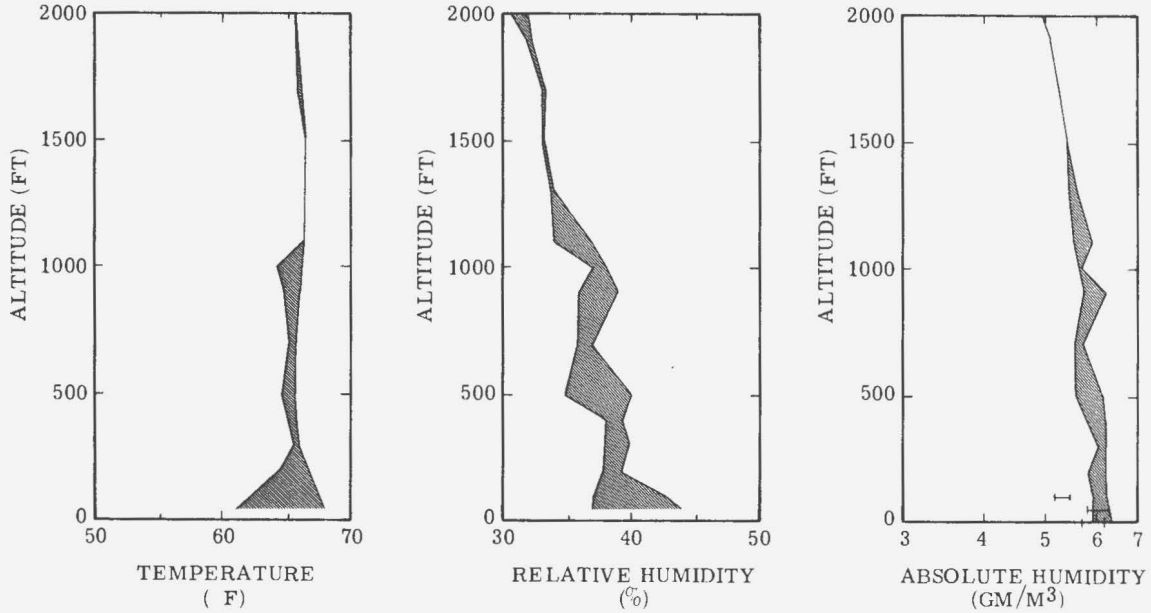

Test Group 4

Figure 11. Aircraft Weather Sounding (Contd)

(e)

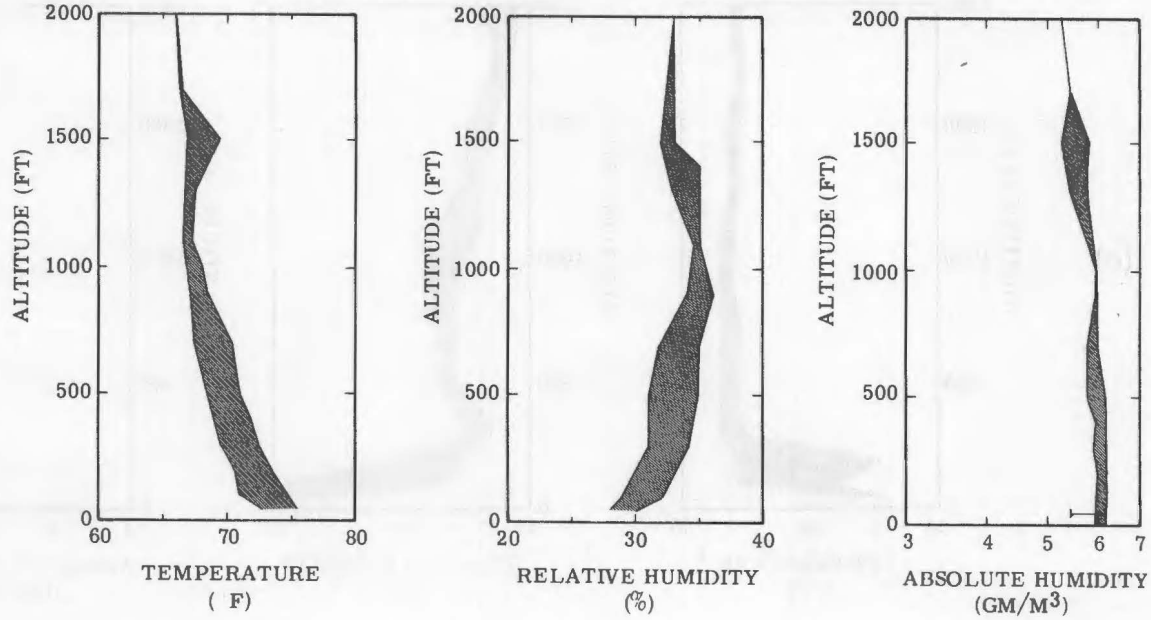

Test Group 5

(f)

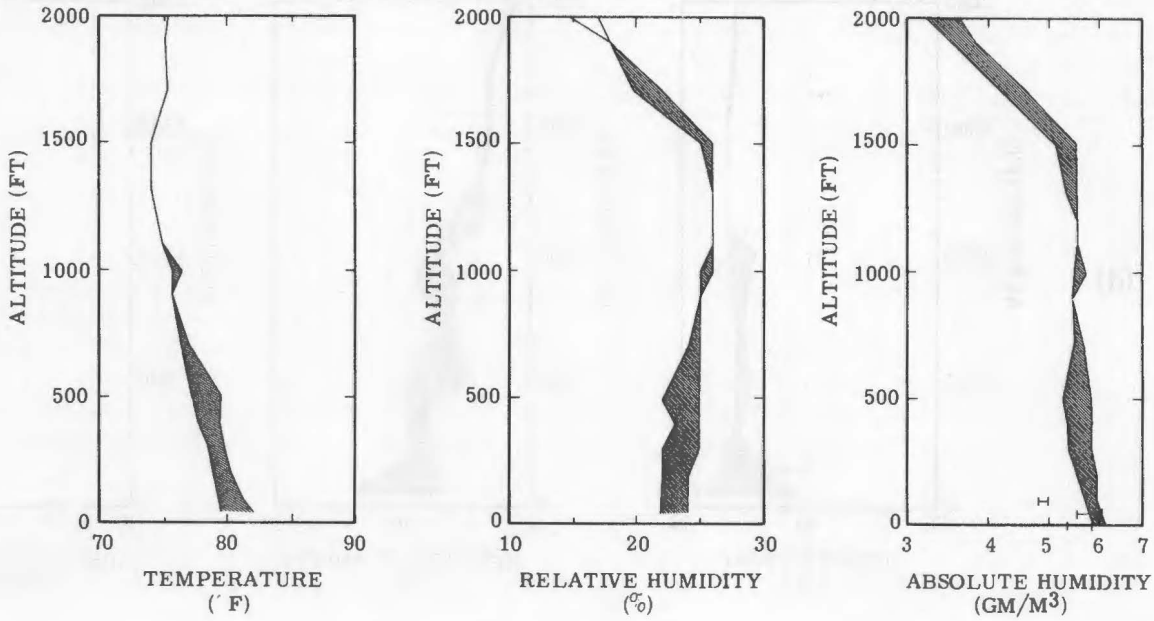

Test Group 6

Figure 11. Aircraft Weather Sounding (Contd)

(g)

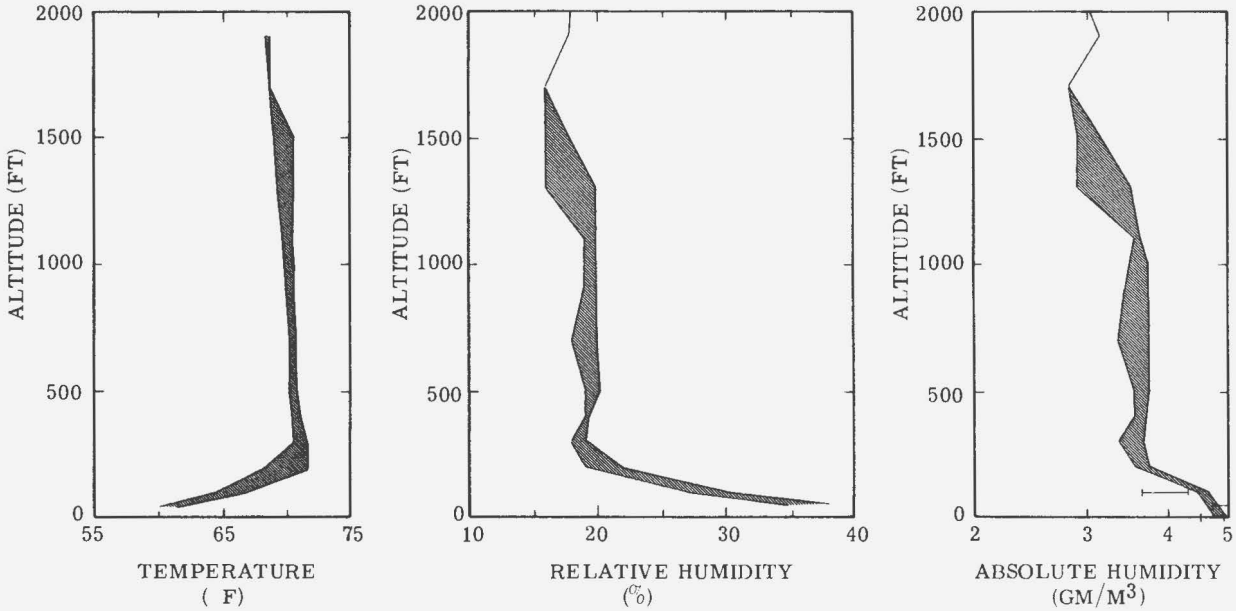

Test Group 7

(h)

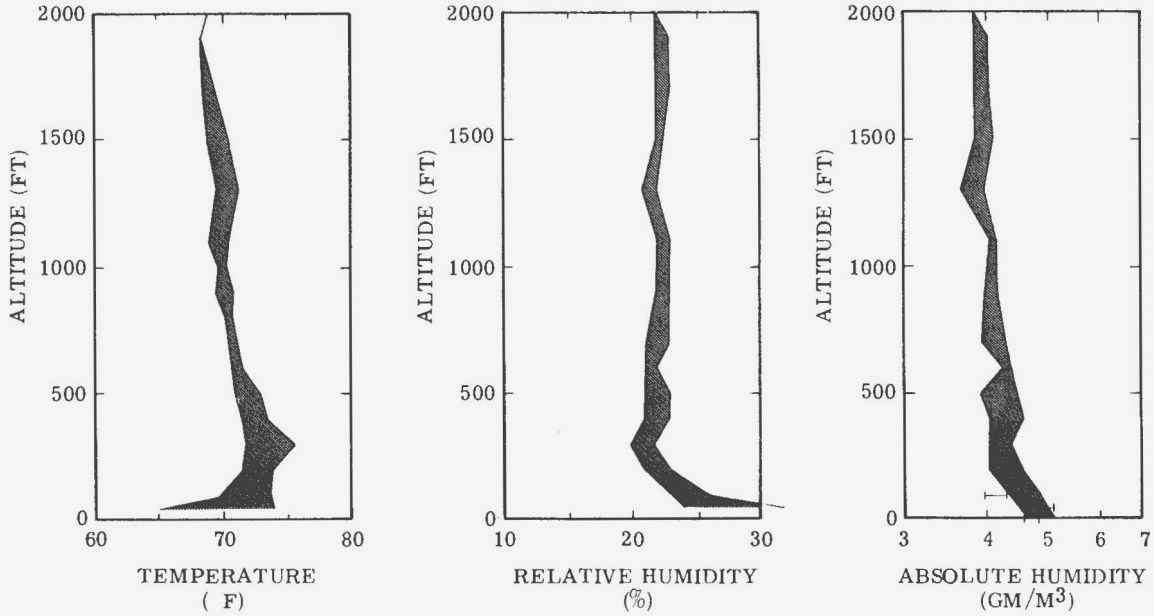

Test Group 8

Figure 11. Aircraft Weather Sounding (Contd)

(i)

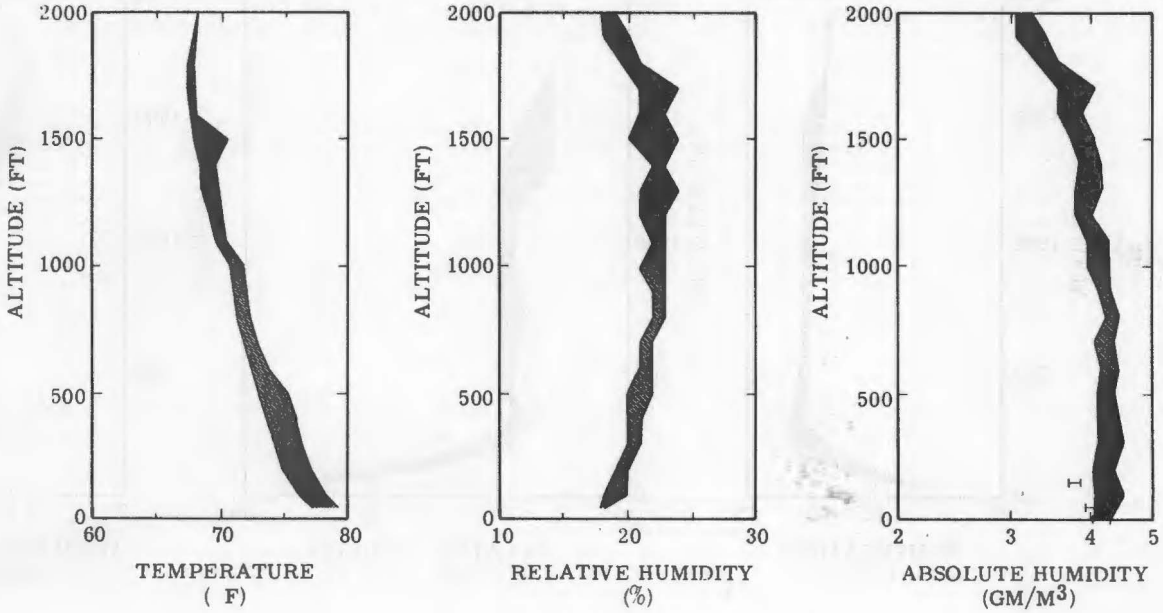

Test Group 9

(j)

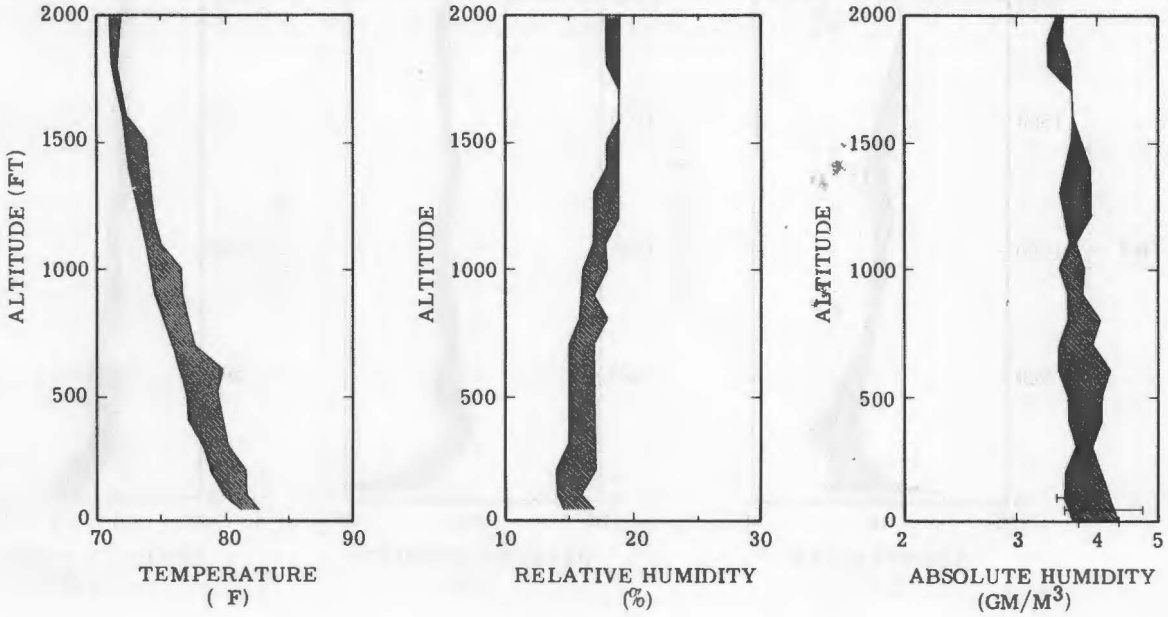

Test Group 10

Figure 11. Aircraft Weather Sounding (Contd)

(a)

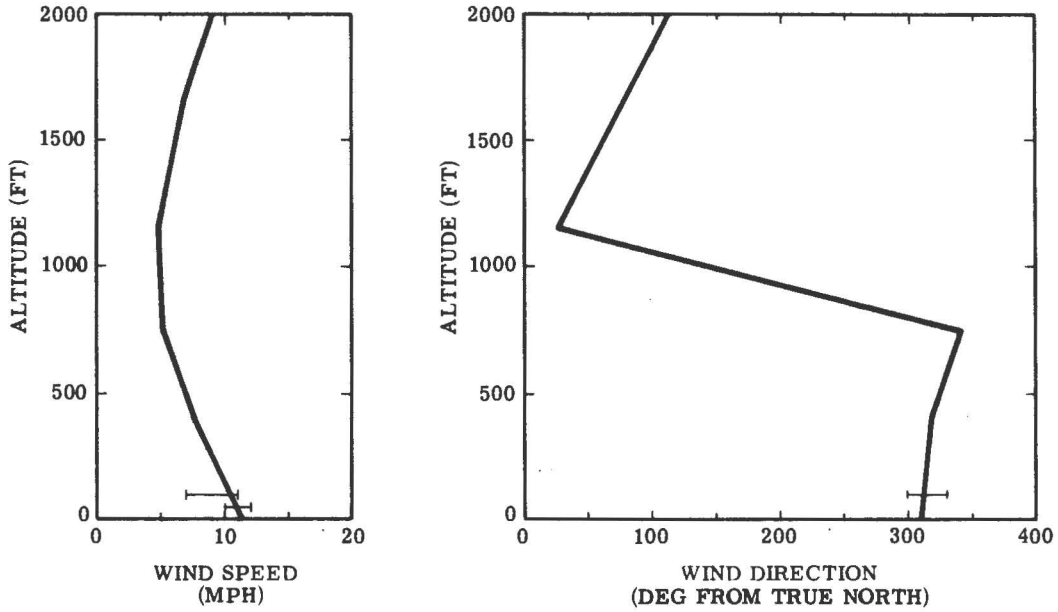

Test Group 2

(b)

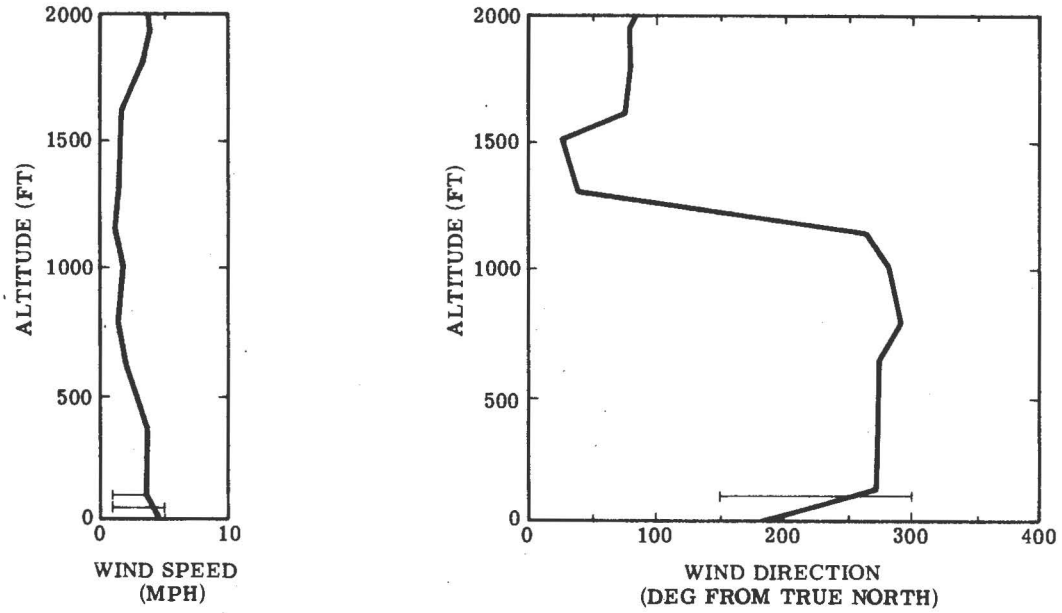

Test Group 4

Figure 12. Radiosonde Weather Sounding

(c)

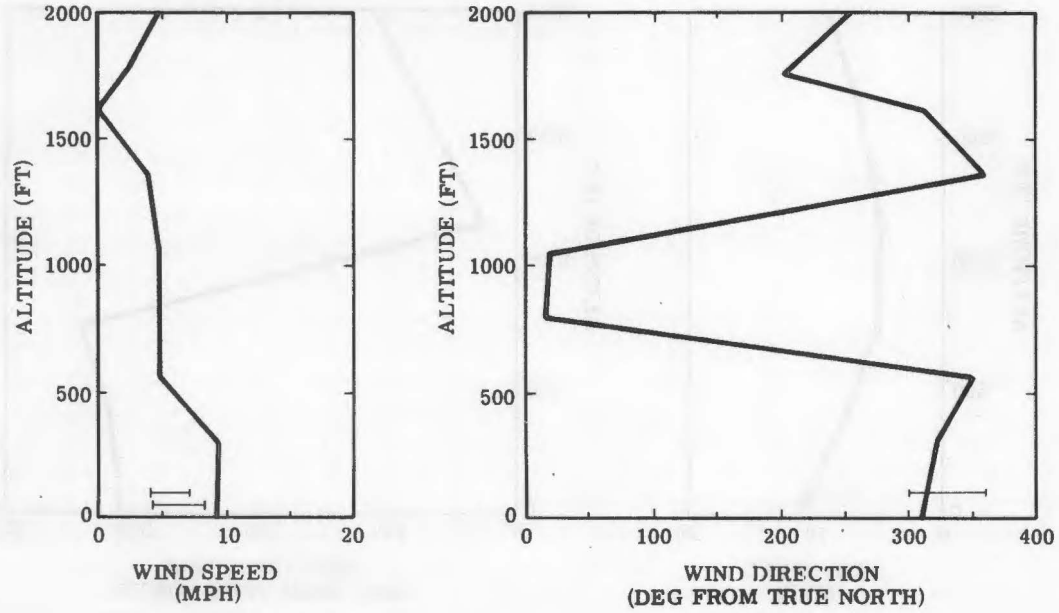

Test Group 5

(d)

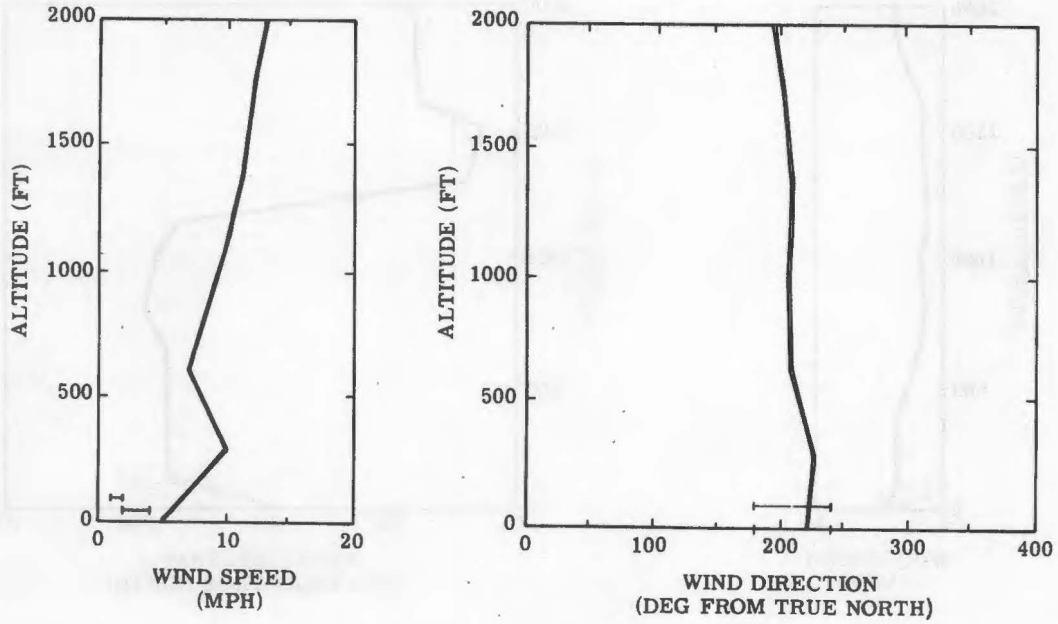

Test Group 6

Figure 12. Radiosonde Weather Sounding (Contd)

(e)

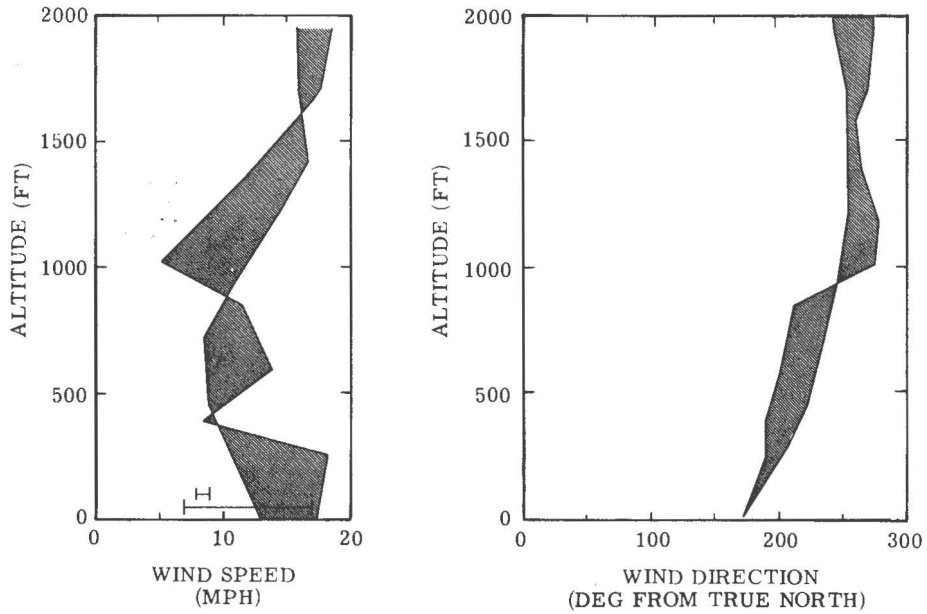

Test Group 7

(f)

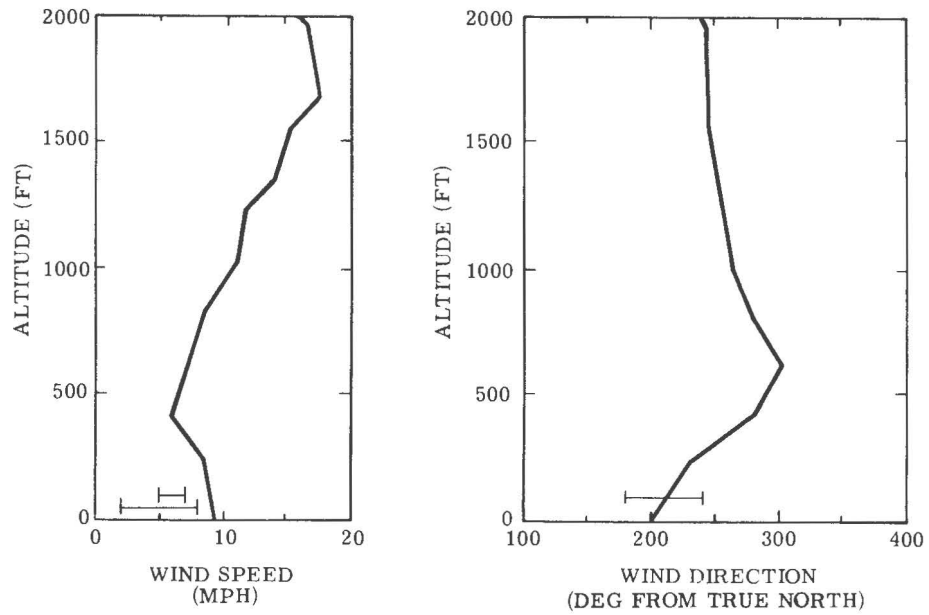

Test Group 8

Figure 12. Radiosonde Weather Sounding (Contd)

(g)

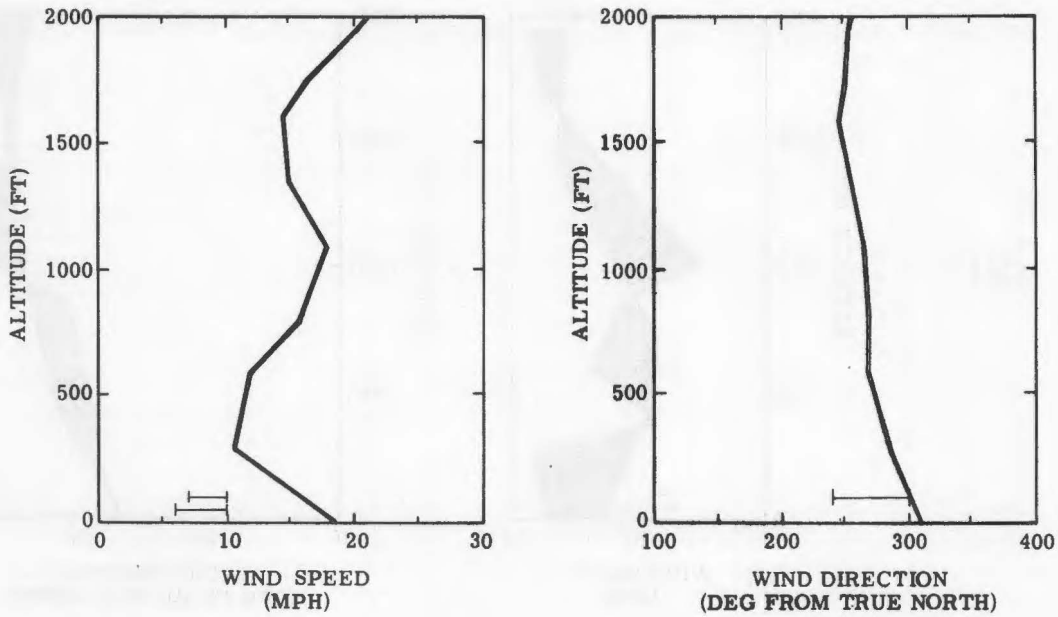

Test Group 9

(h)

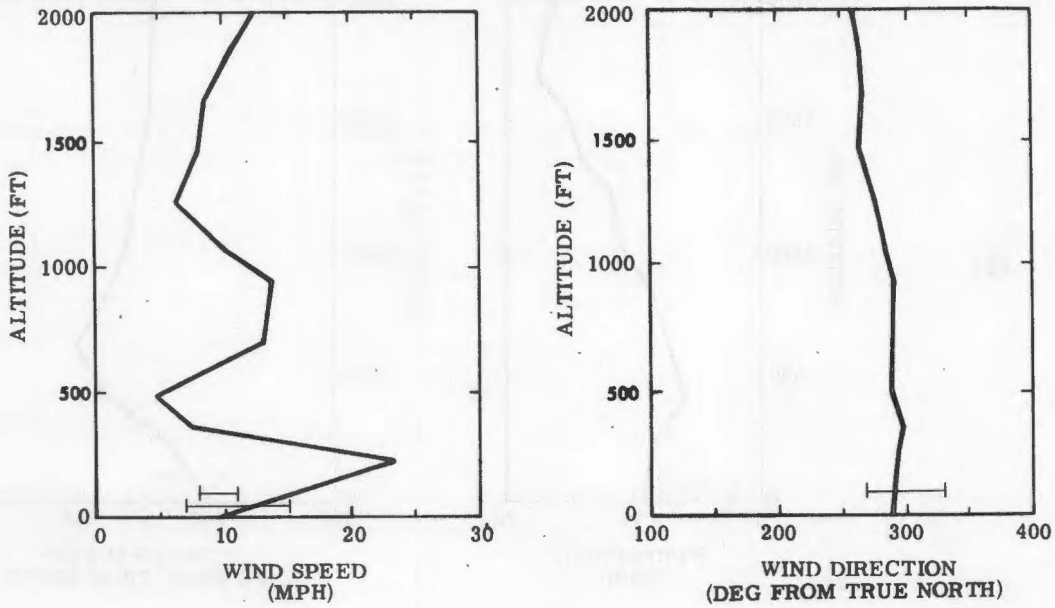

Test Group 10

Figure 12. Radiosonde Weather Sounding (Contd)

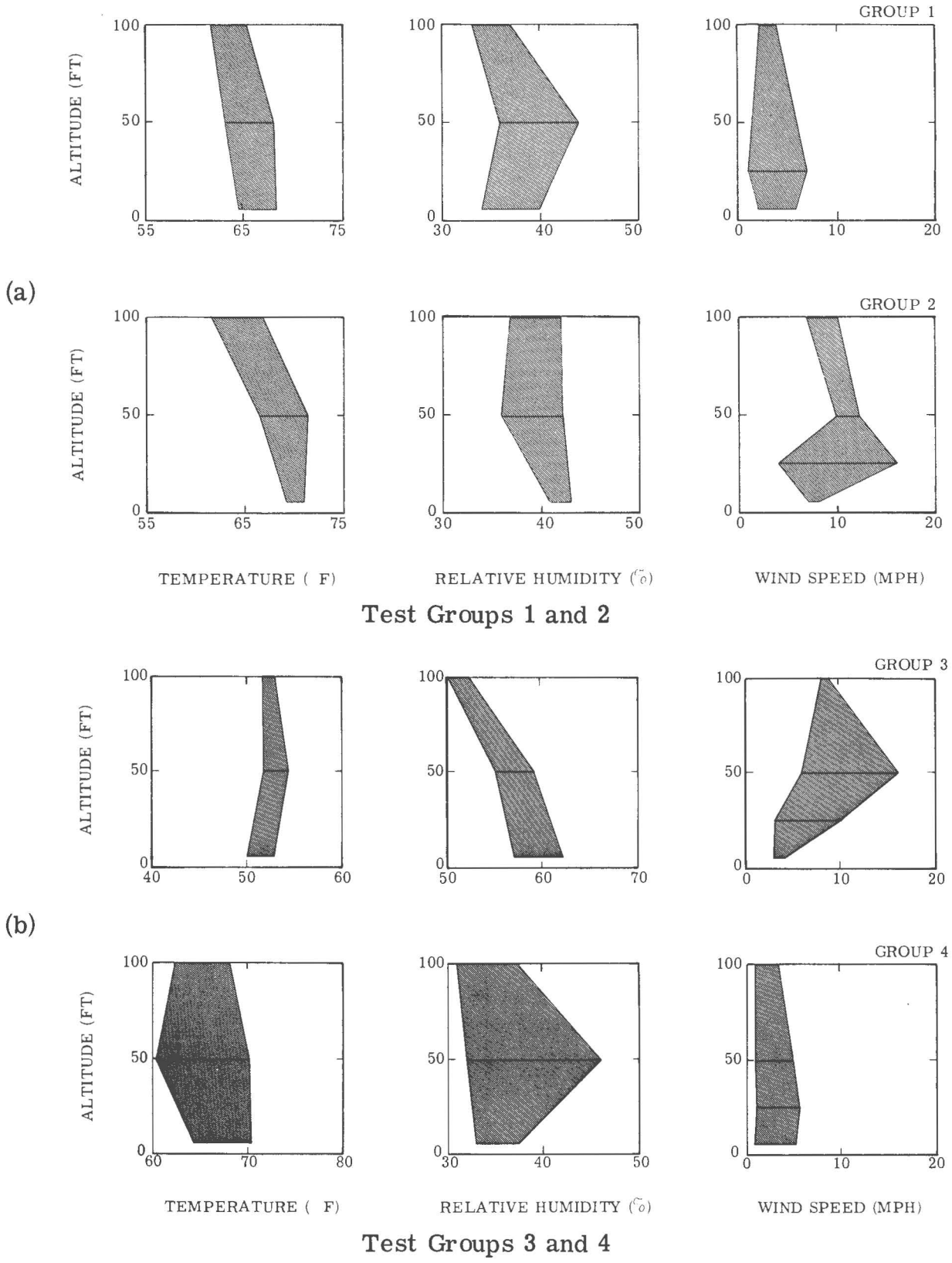

Figure 13. Surface Weather Measurements

(c)

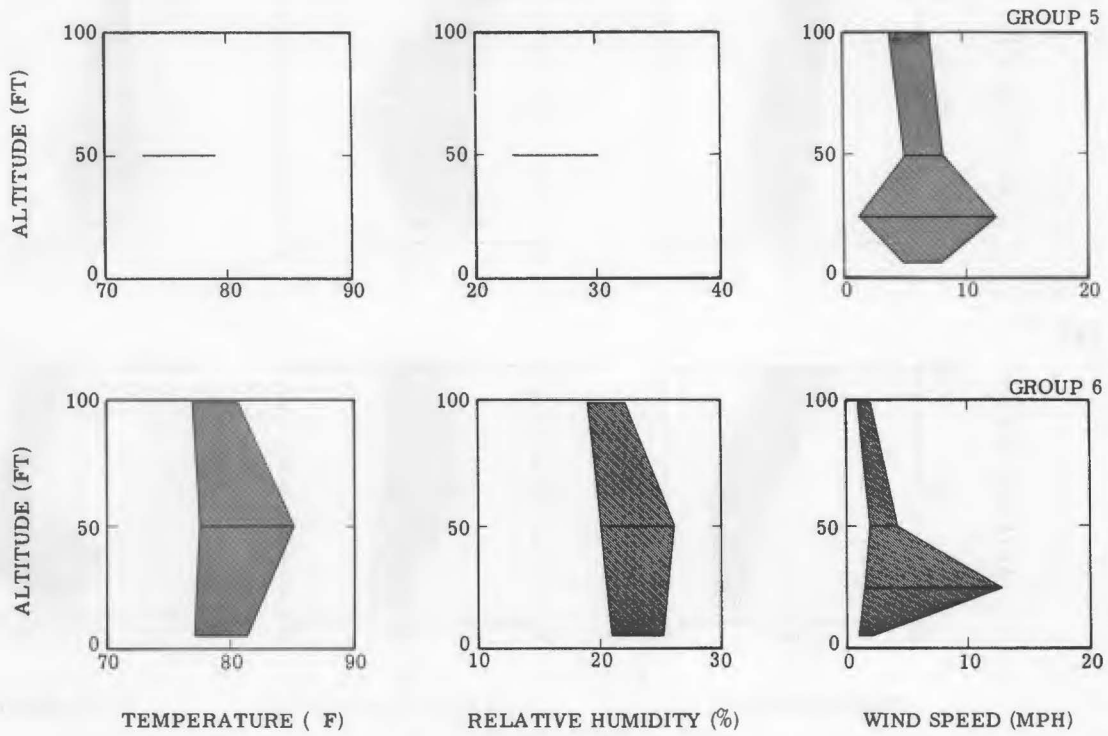

Test Groups 5 and 6

(d)

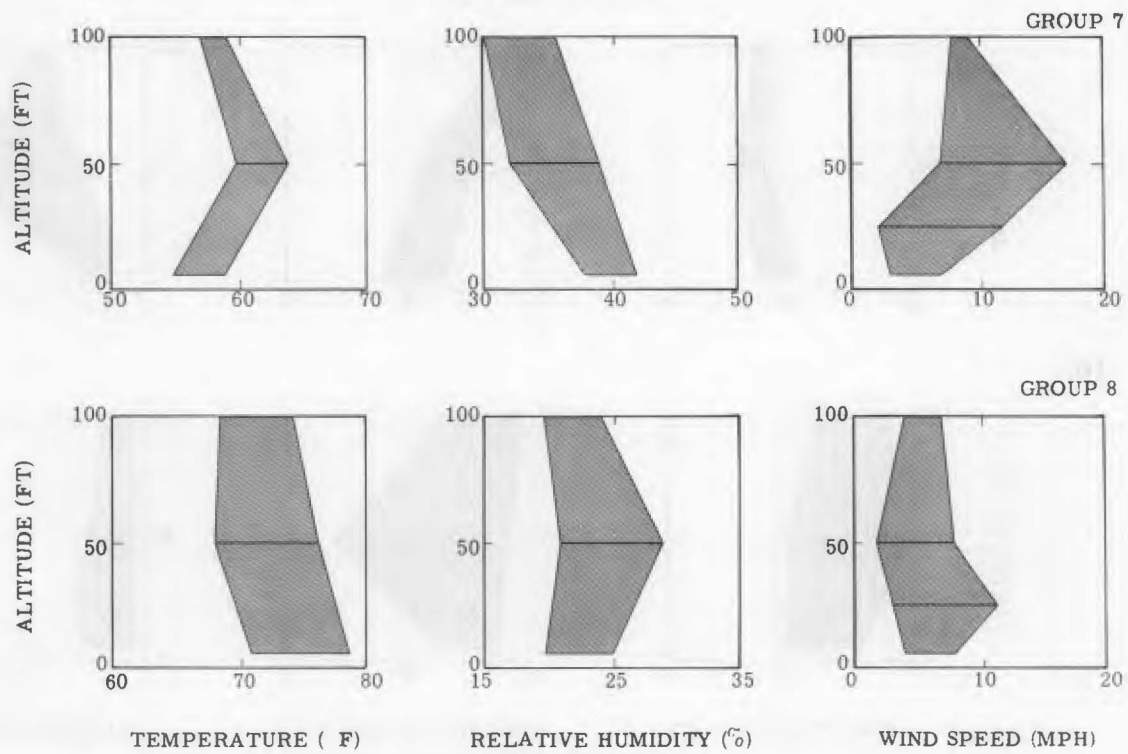

Test Groups 7 and 8

Figure 13. Surface Weather Measurements (Contd)

(e)

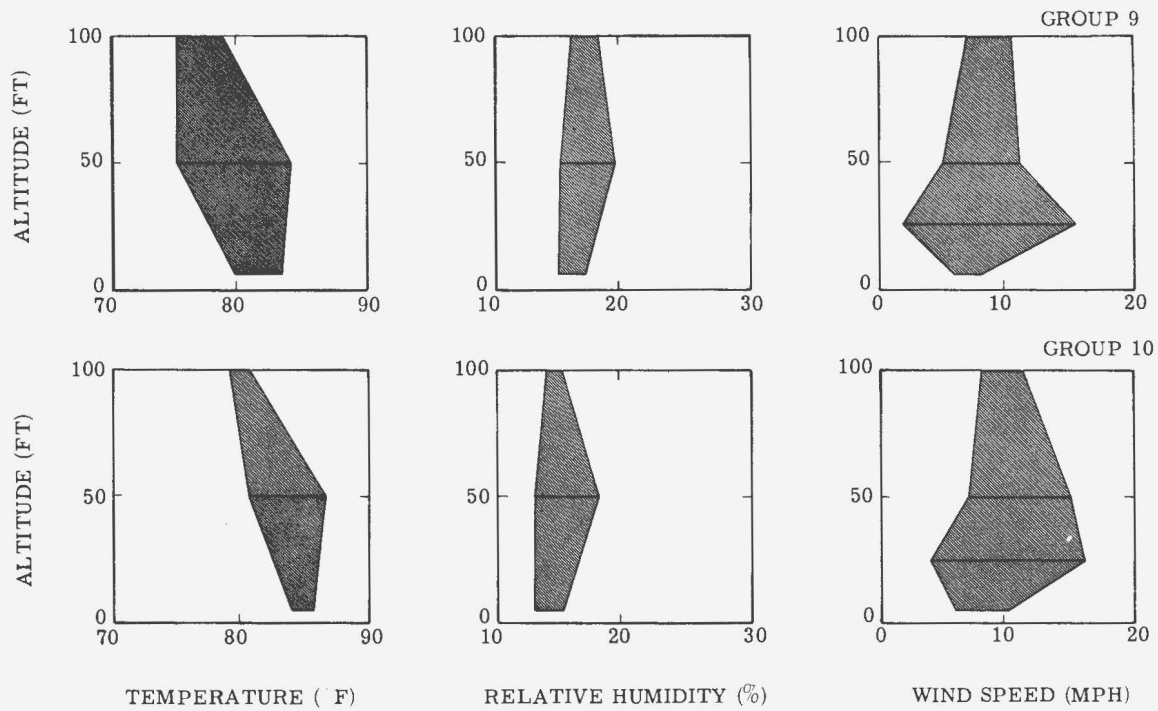

Test Groups 9 and 10

Figure 13. Surface Weather Measurements (Contd)

If the surface data are superimposed over the soundings, it will be apparent that there is poor agreement between the relative humidity at the 100-foot tower level and the weather airplane. The aircraft usually flew the 100-foot segment of the sounding over the asphalt runway. The 100-foot tower, on the other hand, was surrounded by the plowed ground surface. The heating of the runway surface is thought to influence the aircraft weather readings at the 100-foot altitude. An examination of data from the 50-foot towers, each surrounded by different ground cover shows good data agreement over the instrumented area.

Acoustic Data

Of the 88 runs recorded, 78 were used in the final analysis. The other runs were discarded due to tracking problems or bad microphone data. These 78 runs comprise ten test periods, with each test period exhibiting weather conditions of a similar nature. The range of weather conditions for the upper air and the atmospheric absorption coefficients for a typical frequency of 3150 Hz is shown in Figure 14. These data are clearly in the range of interest of lower humidities.

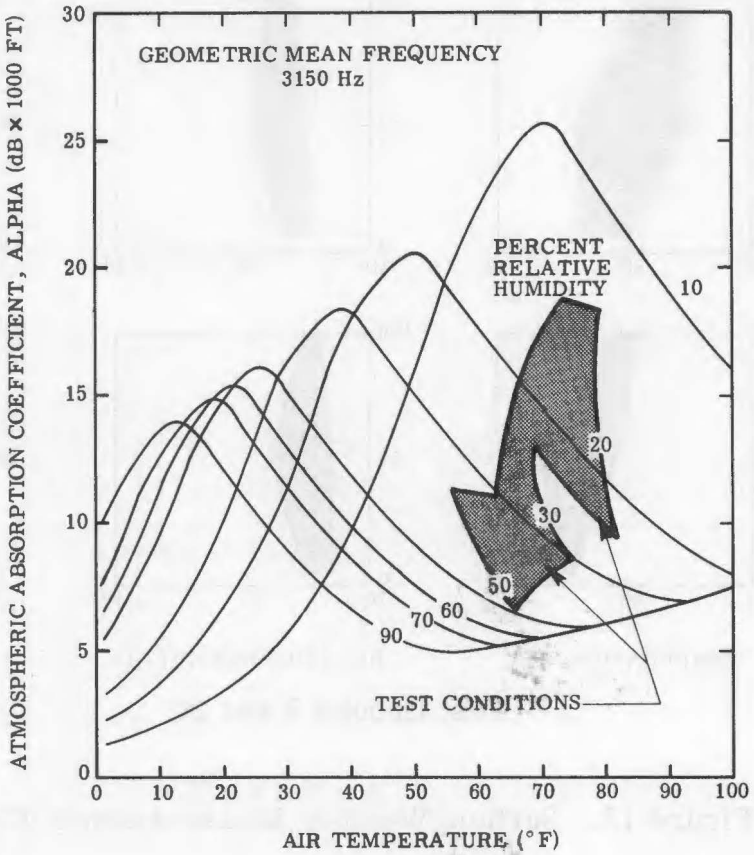

Figure 14. Atmospheric Absorption Coefficients for One-Third Octave Bands of Noise for Different Temperatures and Humidities

Typical normalized spectra obtained at the ground (sites 1, 3, 5, and 7) and 26 feet in the air (sites 2, 4, 6, and 8) for a 1500- and 100-foot altitude flyby are given in Figures 15 and 16. The variation of the spectra at the ground (site 1) and 26 feet in the air (site 2), as a function of nominal test altitude, is shown in Figures 17 and 18, respectively. It can be seen that the high frequency data are limited by the background noise.

The data from the ground microphones exhibited unusual variations from one site to the next which makes it extremely difficult to utilize the results in the calculation of atmospheric absorption. The ground data uncertainty is due in part to the humidity and temperature variations between the ground and the 26-foot microphone.

(a)

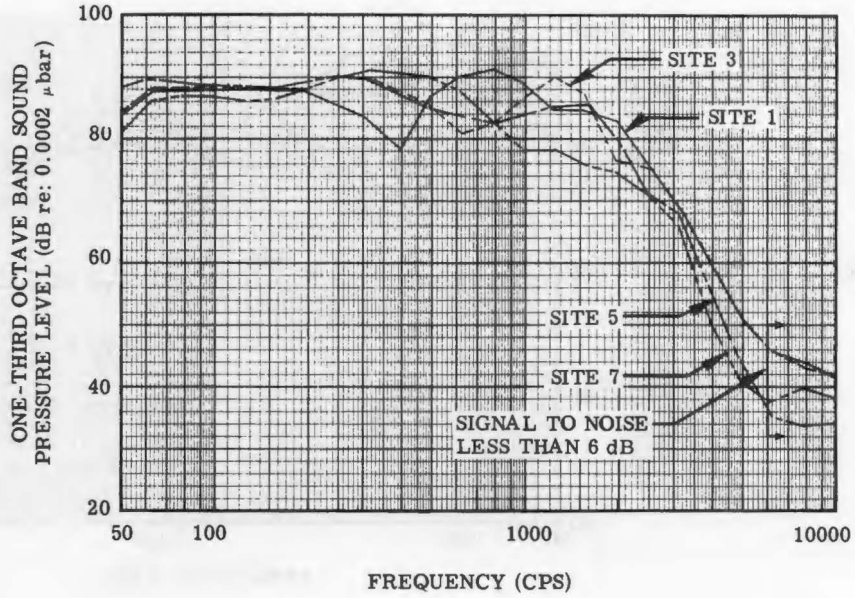

Ground Elevation

(b)

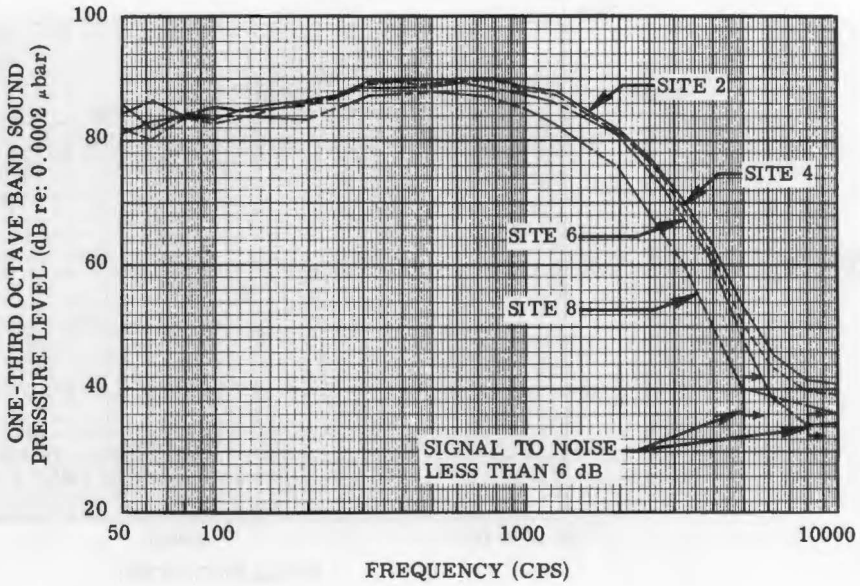

26-Foot Elevation

Figure 15. Variation of Spectra, 1500-Foot Flyby

(a)

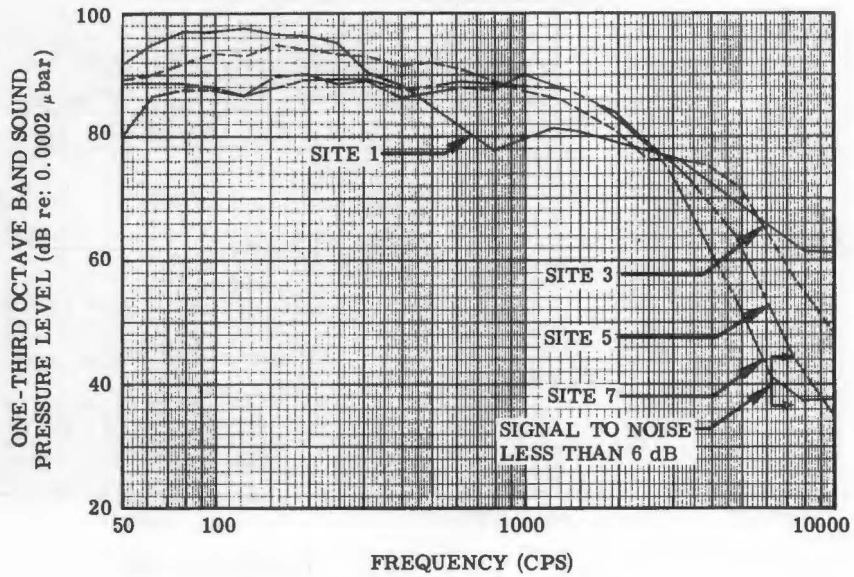

Ground Elevation

(b)

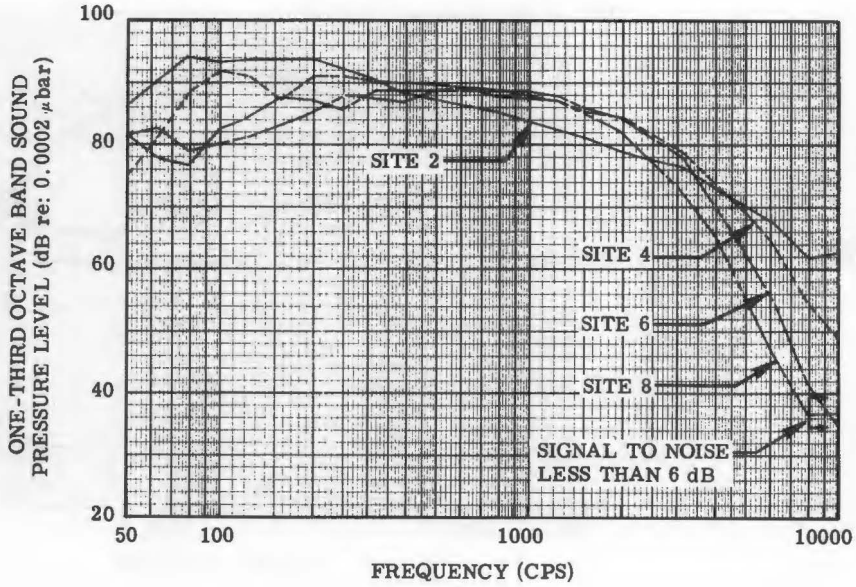

26-Foot Elevation

Figure 16. Variation of Spectra, 100-Foot Flyby

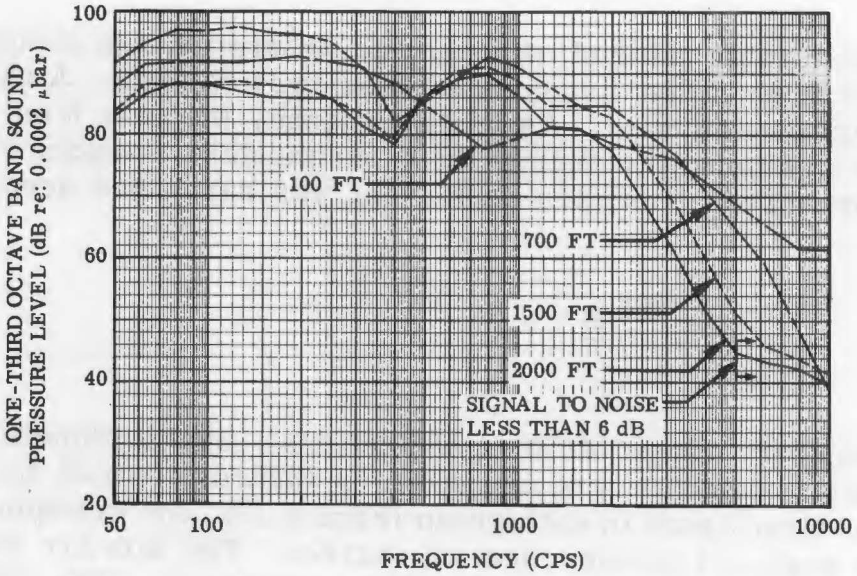

Figure 17. Variation of Spectra at Site 1 as a Function of Test Altitude

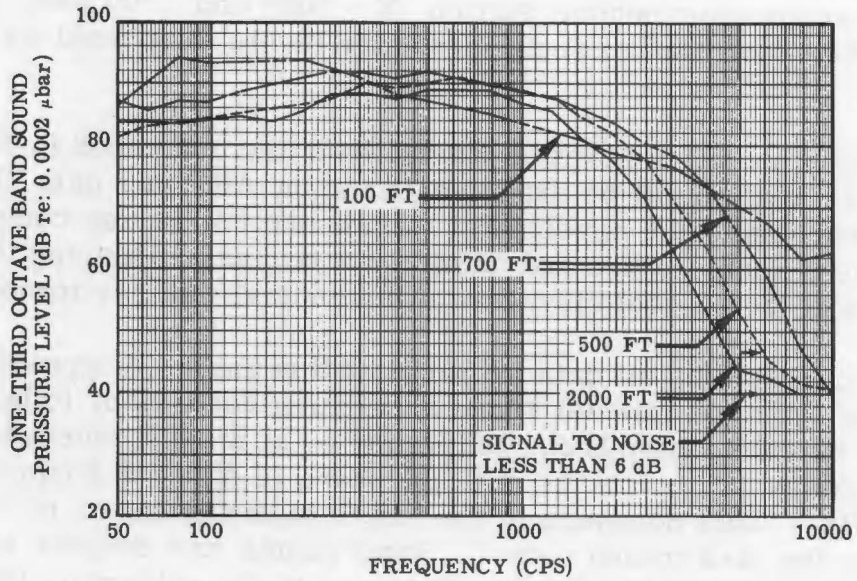

Figure 18. Variation of Spectra at Site 2 as a Function of Test Altitude

An experimental value of atmospheric absorption was computed for the difference in propagation distances between two positions. A variety of microphone pairings was tried. As a consequence, the data from the 26-foot microphones were used to calculate the experimental absorption results given in this report. The absorption coefficient was calculated according to the equation

$$\alpha = \frac{SPL_A - SPL_B}{d_B - d_A}$$

over the frequency range of 50 to 10,000 cps. The arithmetic average of these values was computed and are shown in Figures 19 to 28 for the ten test groups. The first figure in each group (Figure 19a, for example) pertains to an elevation angle (β) greater than 15 degrees. The data are the results of measurements made for three aircraft flyby heights (Z = 700, 1500, and 2000 feet) and all four microphone stations (X = 250, 500, 1000, and 1500 feet), positioned 26 feet above the ground. The three remaining figures in each group (Figures 19b, 19c, and 19d, for example) pertain to elevation angles (β) less than 15 degrees. These data are the results of measurements made for the 100-foot flyby altitude. For example, Figure 19b presents the results of the test data for all microphone stations (X = 250, 500, 1000, and 1500 feet). The remaining two figures (Figures 19c and 19d) present the results of test data for a single microphone station (X = 1000 and 1500 feet, respectively) where the 500-foot station sound pressure levels were used as the baseline values.

The experimental absorption coefficients are compared in Figures 19 to 28 with those that would be expected based on ARP 866 data (Reference 3). The band represents the envelope of air absorption values computed for the observed field temperature and humidity data obtained during the respective test periods at the 50-foot elevation of the central weather tower.

An examination of all data for an elevation angle (β) greater than 15 degrees shows the experimental sound absorption coefficient to be greater than the band of data computed from Reference 3, at most frequencies. The test data consistently fall below the ARP 866 band of data for frequencies greater than 5000 Hz. This downturn in the test data is attributed to the test signal approaching the background noise. Some values are subject to large error due to the limited number of data points and to the extremely low humidities. Low frequency data from 50 to 100 Hz indicate a tendency to fall below the calculated zero absorption coefficient.

The test data for an elevation angle (β) less than 15 degrees, and for all microphones (Figure 19b, for example), generally fall below the calculated

ARP 866 data, except for frequencies less than 200 Hz. Again, the downturn in data is exhibited for frequencies greater than 6300 Hz.

The data shown in Figures 19c and 19d, for example, for narrower ranges of angle of elevation indicate considerably larger scatter for frequencies less than 500 Hz. The greater scatter is due to the use of only two microphones.

The data given for an elevation angle less than 15 degrees should include the effects of extra ground attenuation. A comparison of data from Figures 19a and 19b, for example, would indicate that extra ground attenuation increases the sound absorption coefficient for frequencies less than 200 Hz. However, for frequencies greater than 200 Hz, the sound absorption coefficient in Figure 19b is less than that shown in Figure 19a.

(a)

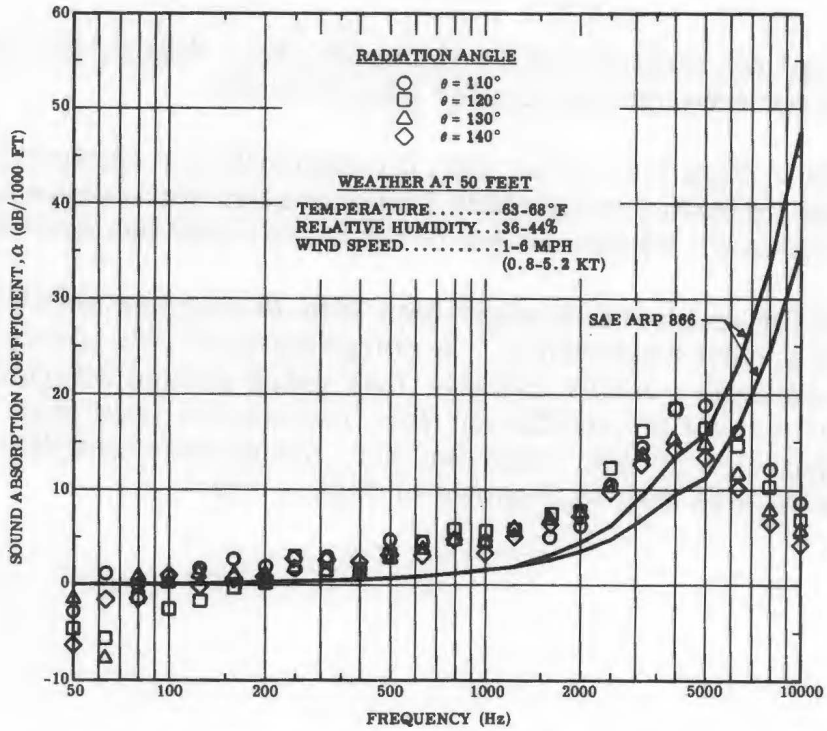

$\beta > 15°$; Z $\geq$ 700 Feet; X = 250, 500, 1000, 1500 Feet

(b)

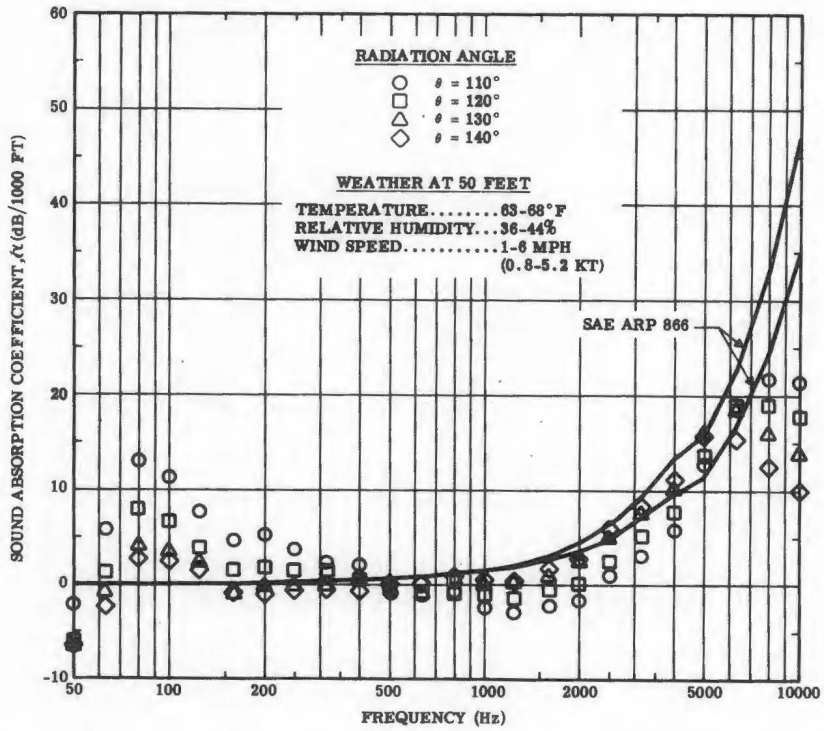

$\beta < 15°$; Z = 100 Feet; X = 250, 500, 1000, 1500 Feet

Figure 19. Sound Absorption Coefficients, Test Group 1

(c)

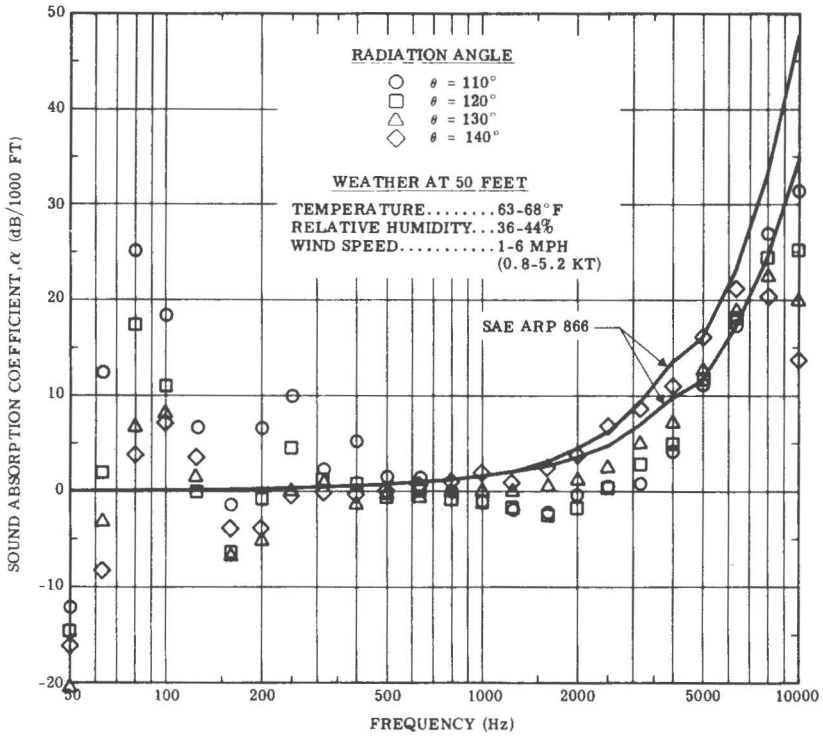

$\beta < 15°$; Z = 100 Feet; X = 500, 1000 Feet

(d)

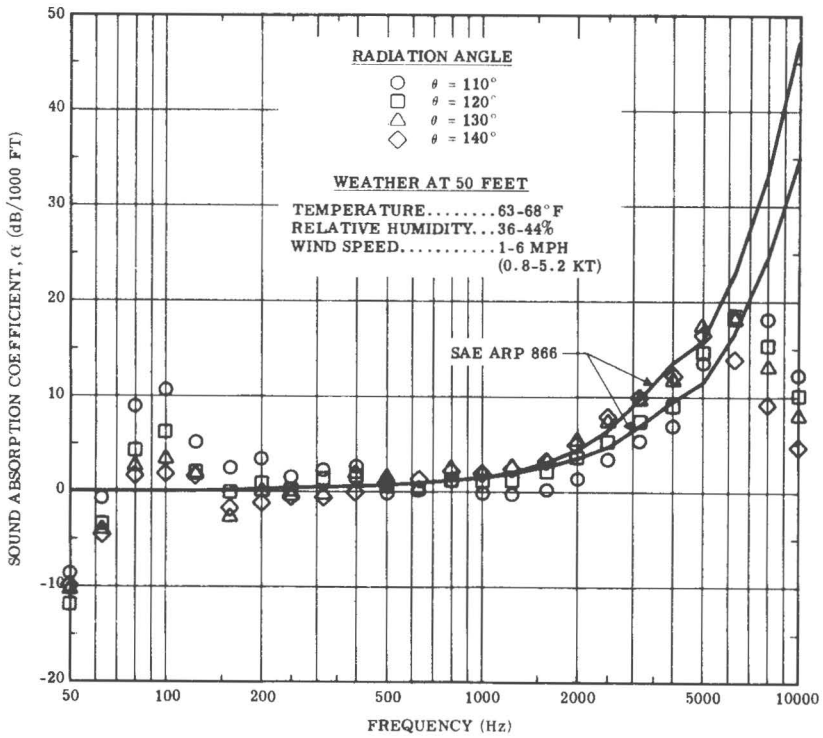

$\beta < 15°$; Z = 100 Feet; X = 500, 1500 Feet

Figure 19. Sound Absorption Coefficients, Test Group 1 (Contd)

(a)

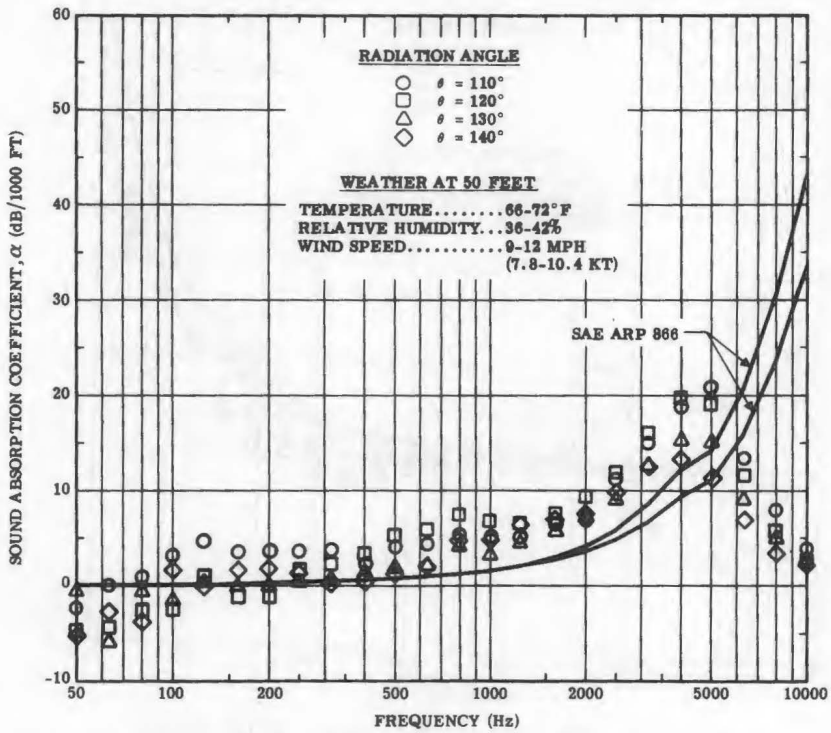

$\beta > 15°$; Z $\geqq$ 700 Feet; X = 250, 500, 1000, 1500 Feet

(b)

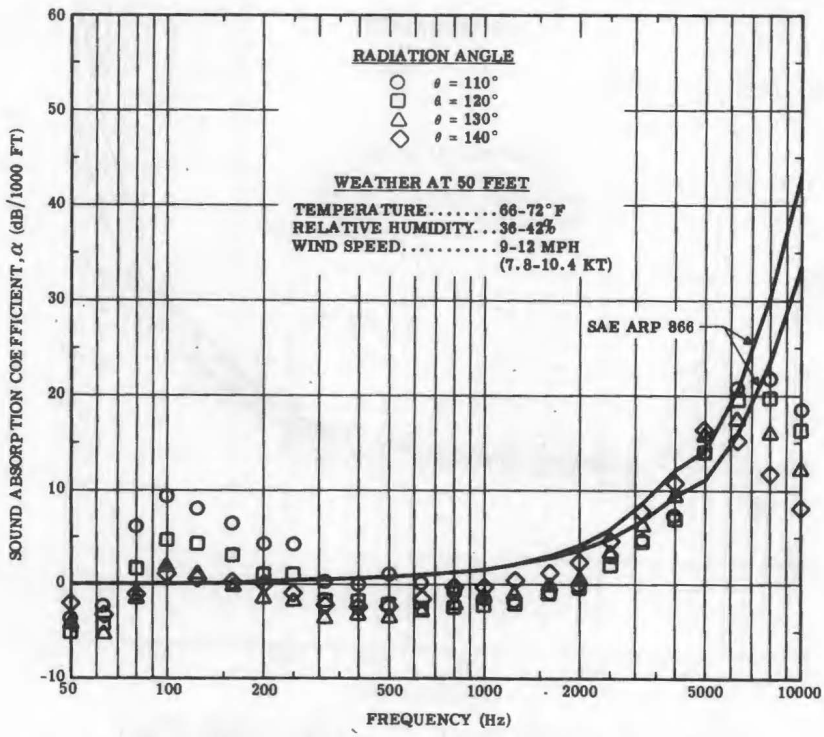

$\beta < 15°$; Z = 100 Feet; X = 250, 500, 1000, 1500 Feet

Figure 20. Sound Absorption Coefficients, Test Group 2

(c)

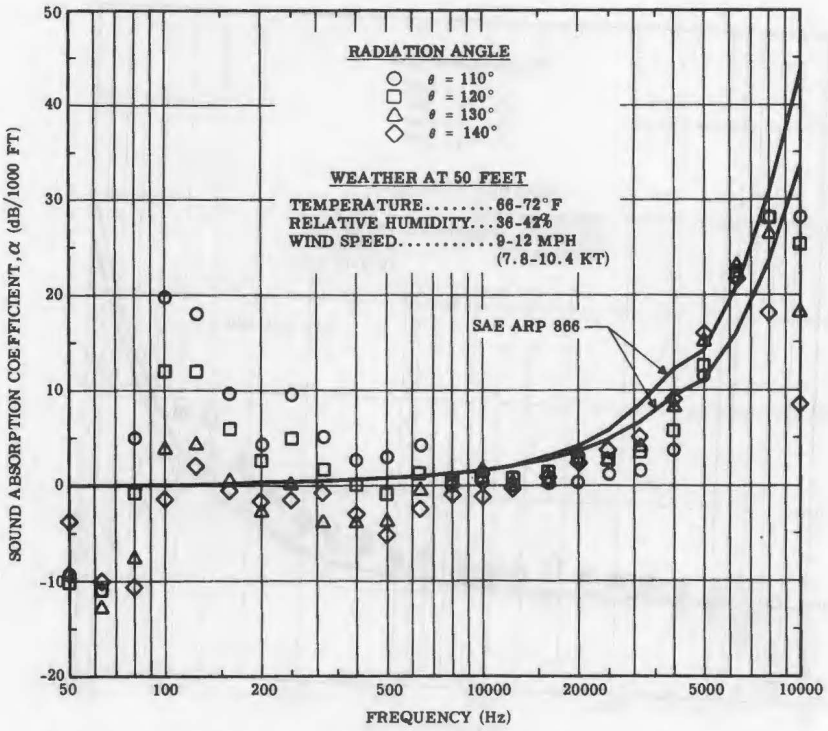

$\beta < 15°$; Z = 100 Feet; X = 500, 1000 Feet

(d)

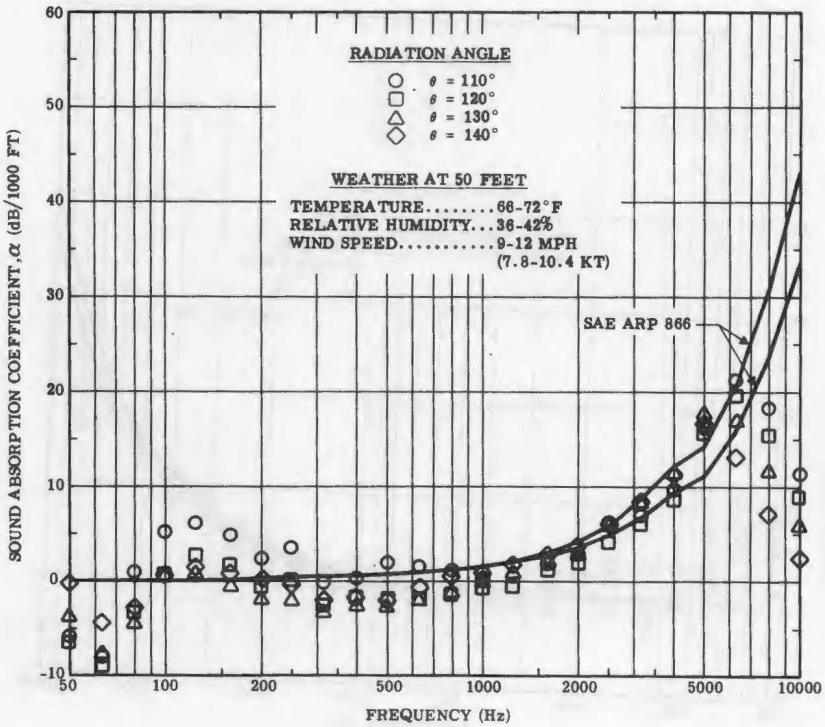

$\beta < 15°$; Z = 100 Feet; X = 500, 1500 Feet

Figure 20. Sound Absorption Coefficients, Test Group 2 (Contd)

(a)

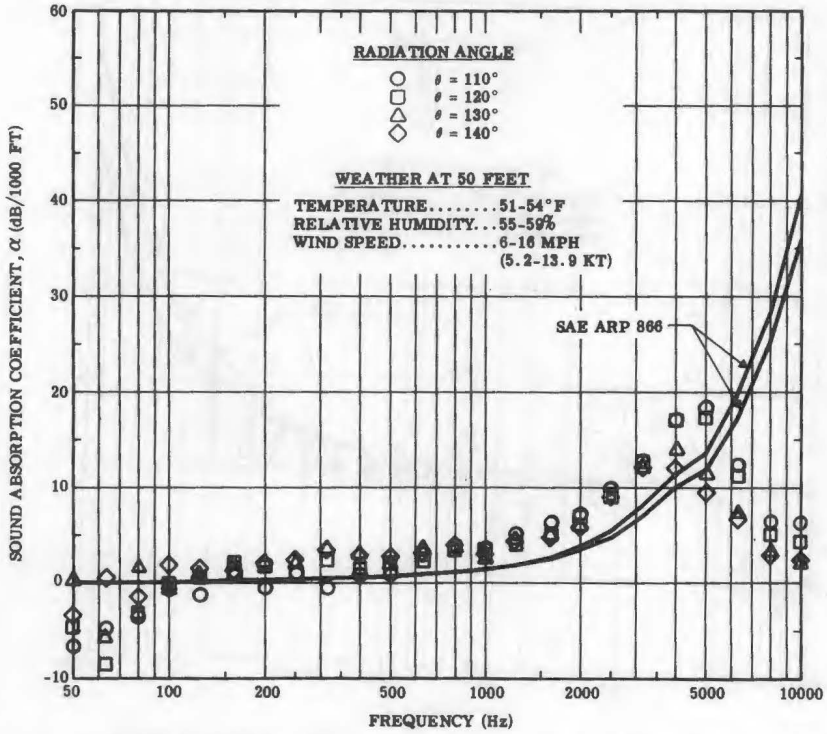

$\beta > 15°$; Z ≥ 700 Feet; X = 250, 500, 1000, 1500 Feet

(b)

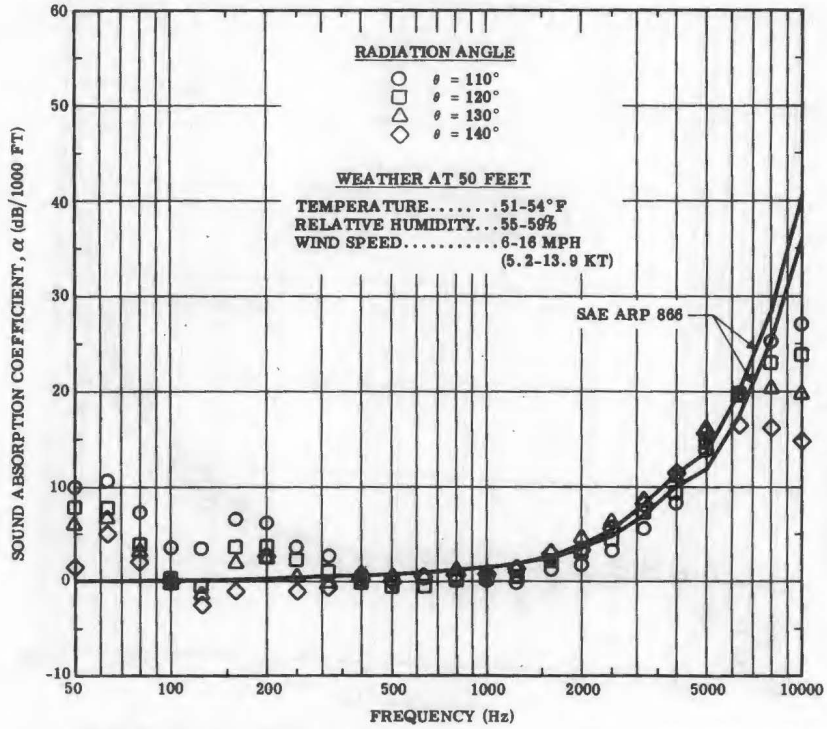

$\beta < 15°$; Z = 100 Feet; X = 250, 500, 1000, 1500 Feet

Figure 21. Sound Absorption Coefficients, Test Group 3

(c)

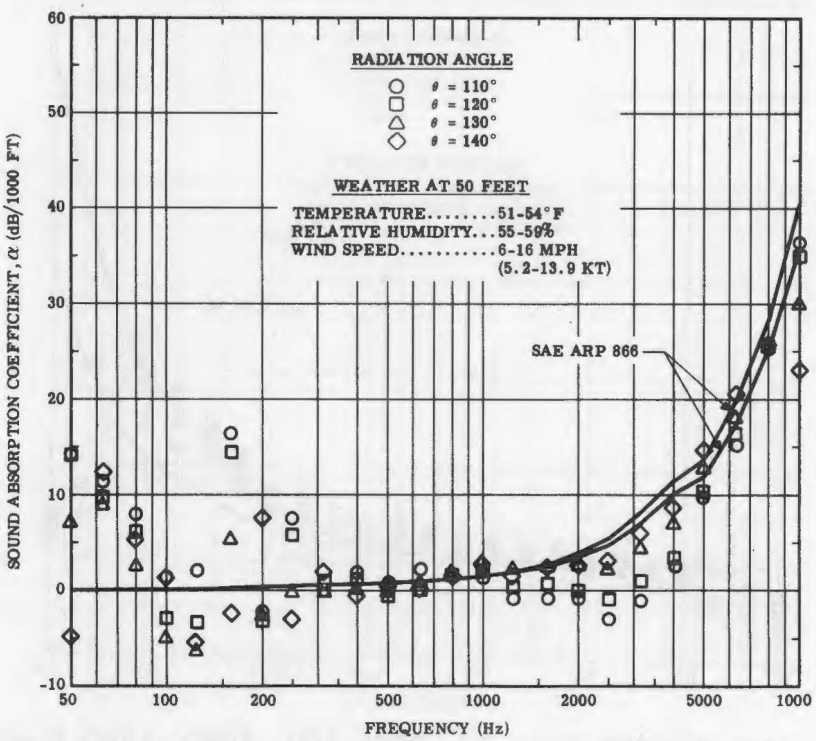

$\beta < 15°$; Z = 100 Feet; X = 500, 1000 Feet

(d)

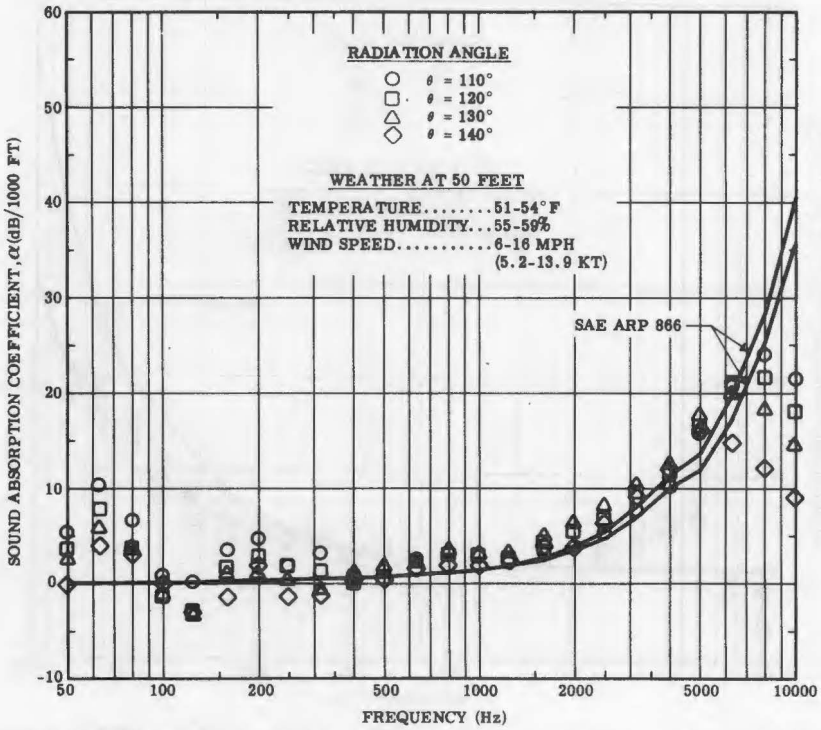

$\beta < 15°$; Z = 100 Feet; X = 500, 1500 Feet

Figure 21. Sound Absorption Coefficients, Test Group 3 (Contd)

(a)

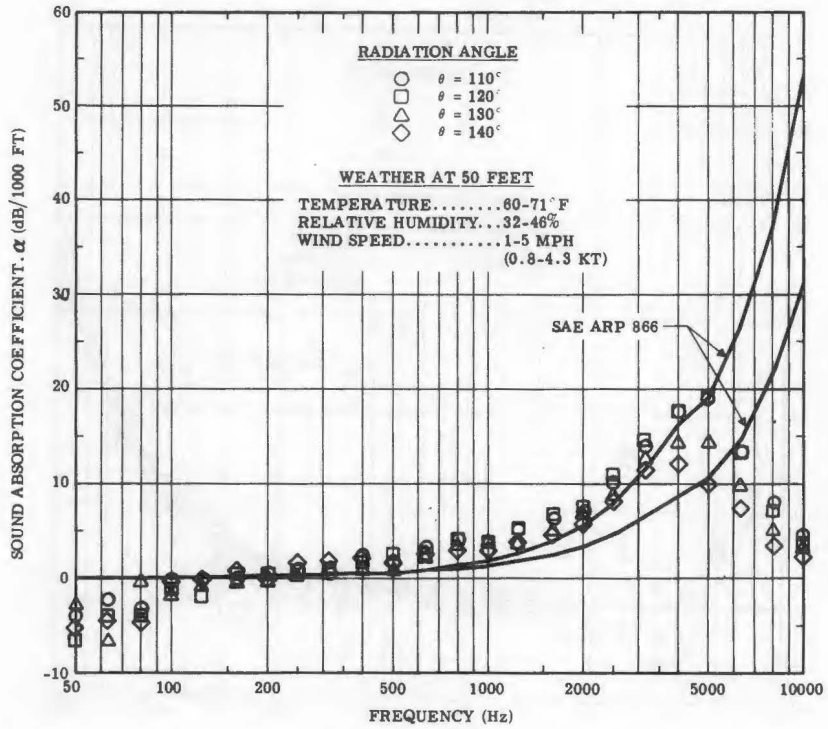

$\beta > 15°$; Z ≥ 700 Feet; X = 250, 500, 1000, 1500 Feet

(b)

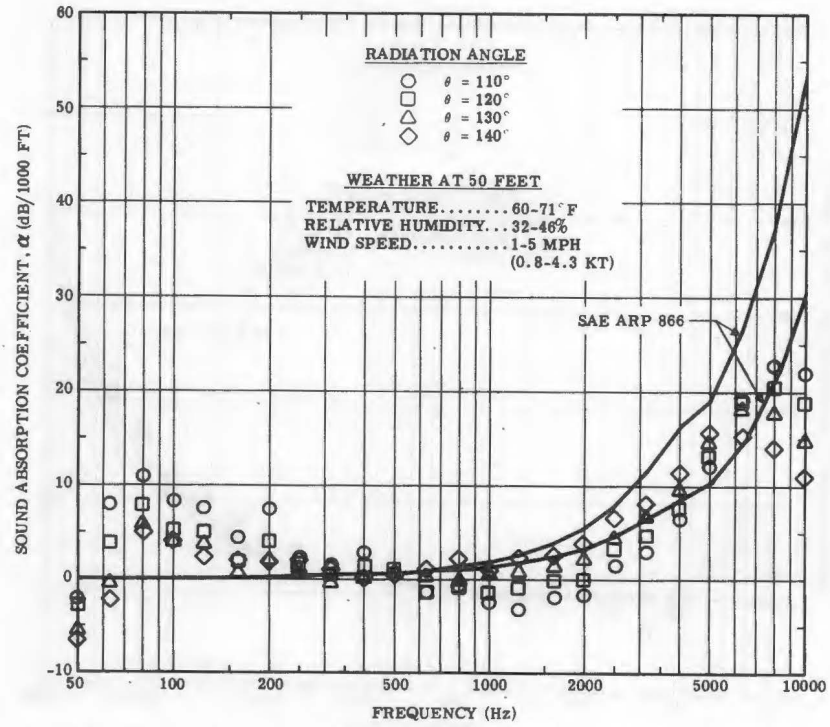

$\beta < 15°$; Z = 100 Feet; X = 250, 500, 1000, 1500 Feet

Figure 22. Sound Absorption Coefficients, Test Group 4

(c)

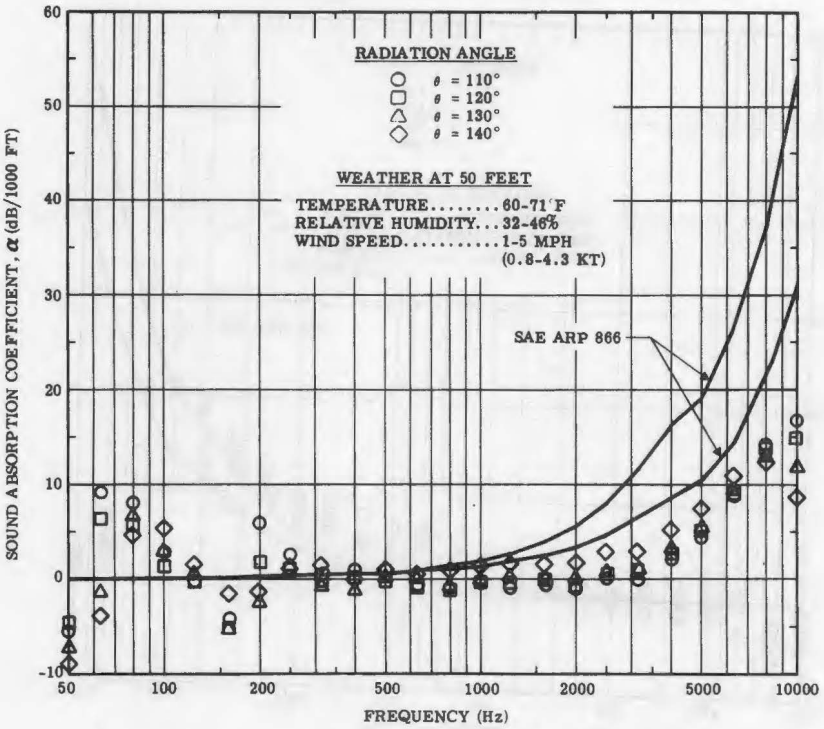

$\beta < 15°$; Z = 100 Feet; X = 500, 1000 Feet

(d)

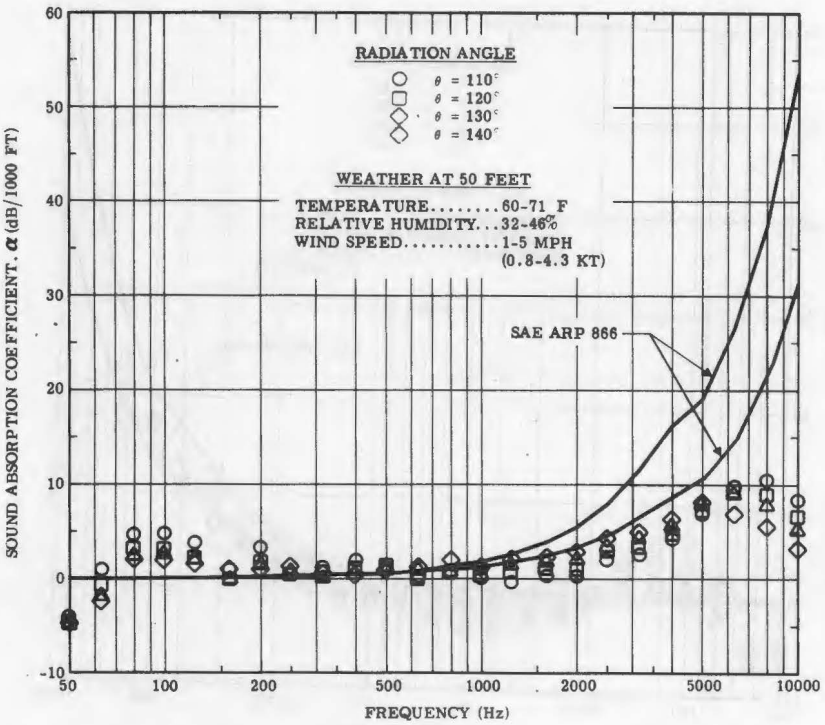

$\beta < 15°$; Z = 100 Feet; X = 500, 1500 Feet

Figure 22. Sound Absorption Coefficients, Test Group 4 (Contd)

(a)

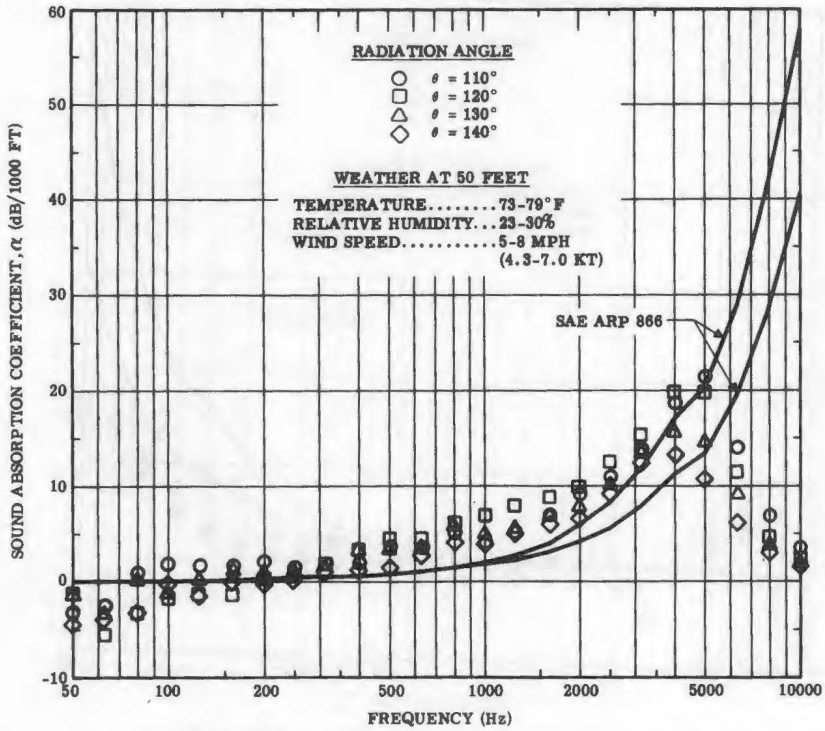

$\beta > 15°$; Z $\geq$ 700 Feet; X = 250, 500, 1000, 1500 Feet

(b)

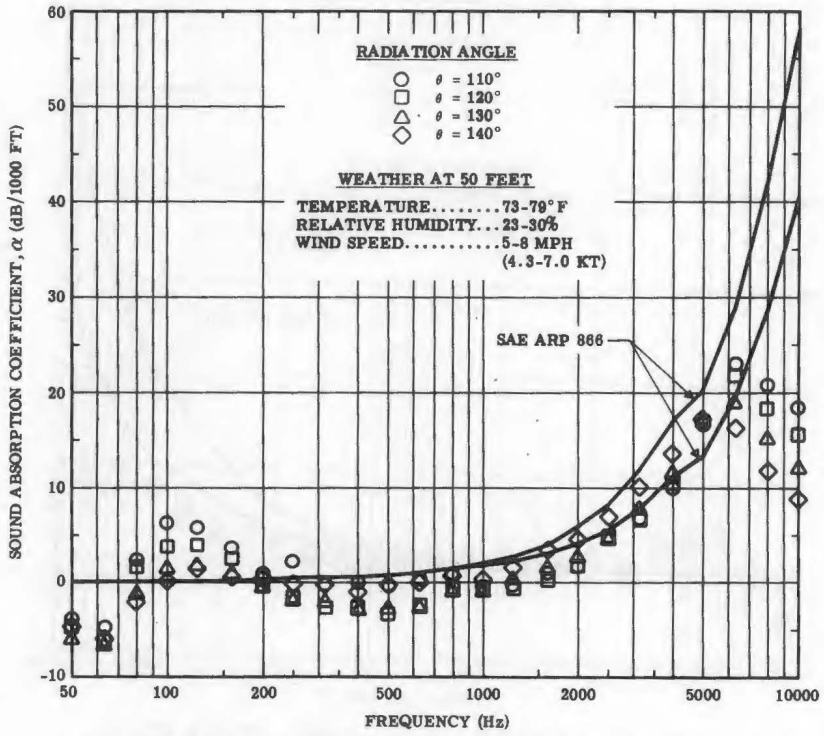

$\beta < 15°$; Z = 100 Feet; X = 250, 500, 1000, 1500 Feet

Figure 23. Sound Absorption Coefficients, Test Group 5

(c)

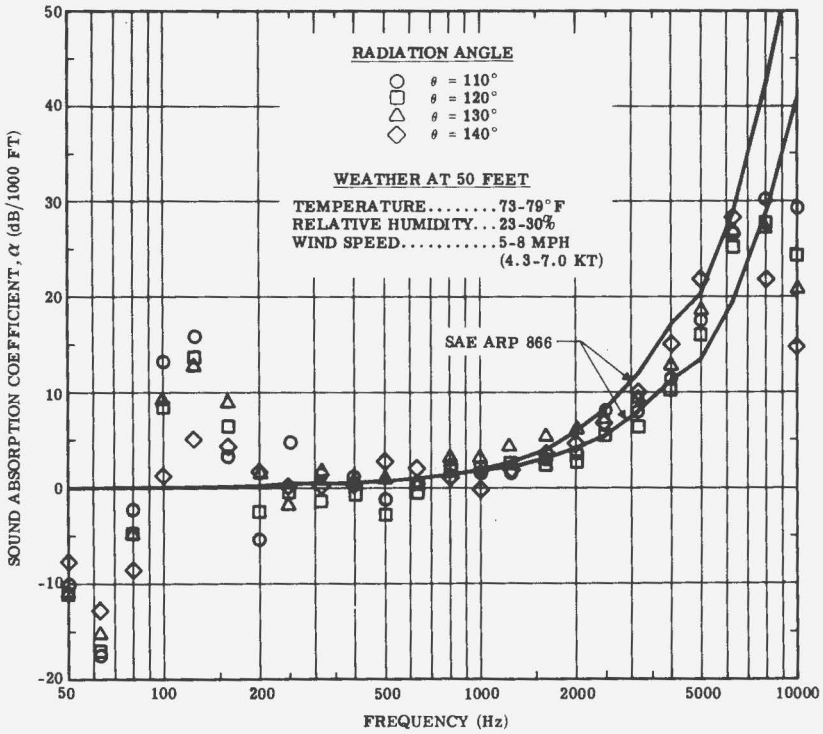

$\beta < 15°$; Z = 100 Feet; X = 500, 1000 Feet

(d)

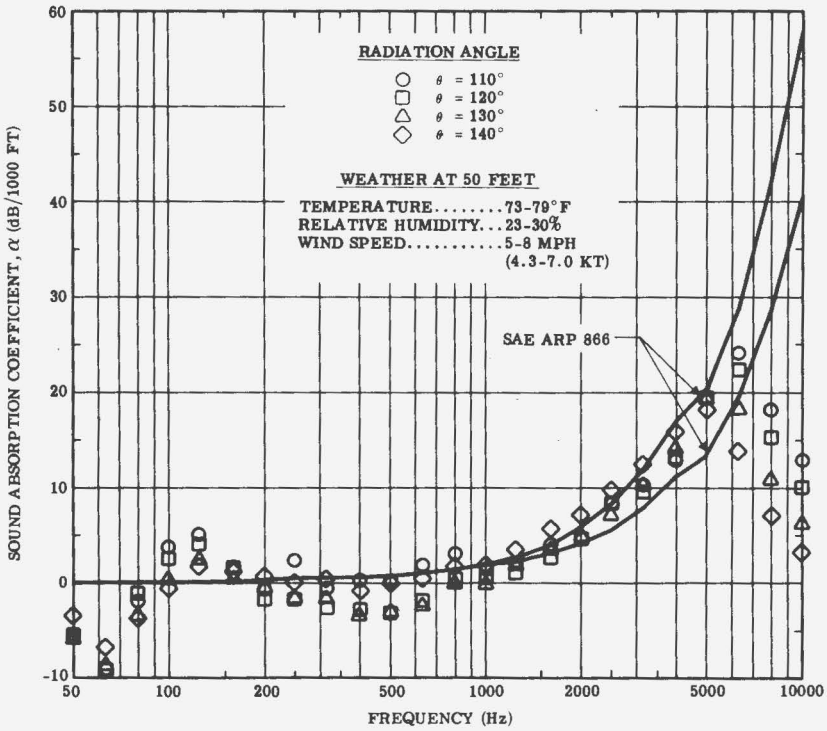

$\beta < 15°$; Z = 100 Feet; X = 500, 1500 Feet

Figure 23. Sound Absorption Coefficients, Test Group 5 (Contd)

(a)

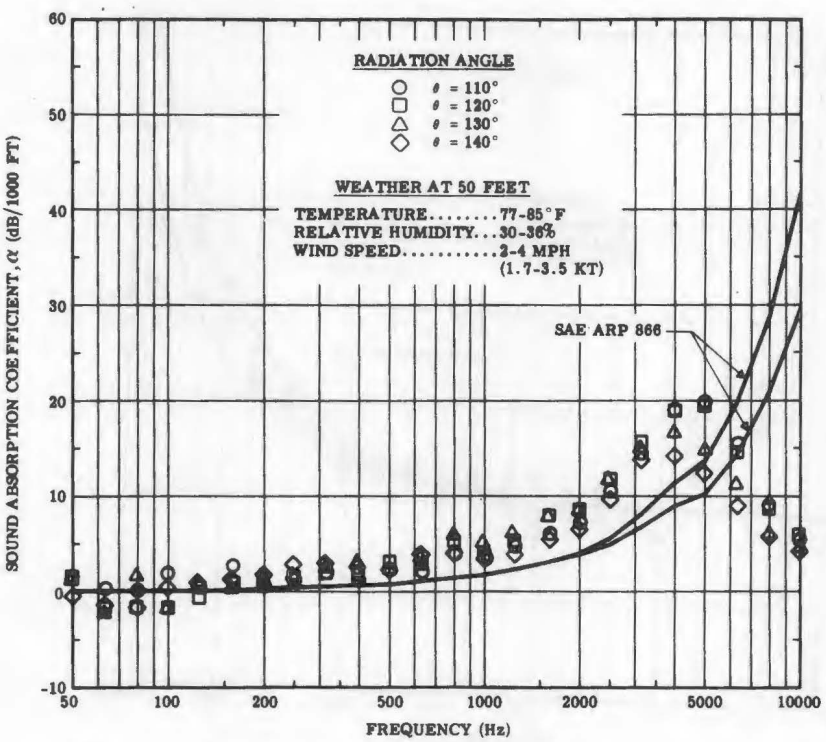

$\beta > 15°$; Z $\geq$ 700 Feet; X = 250, 500, 1000, 1500 Feet

(b)

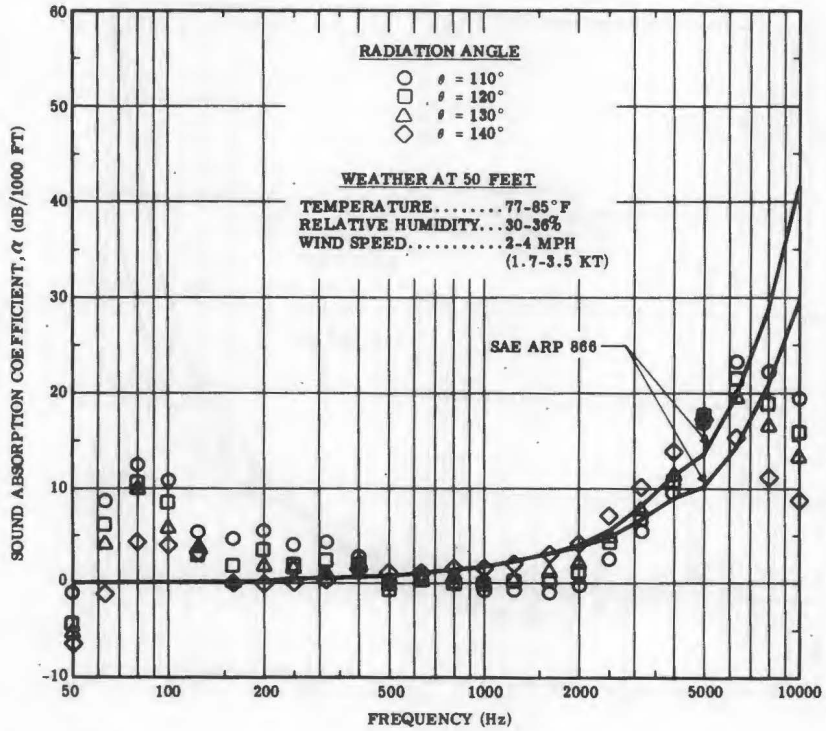

$\beta < 15°$; Z = 100 Feet; X = 250, 500, 1000, 1500 Feet

Figure 24. Sound Absorption Coefficients, Test Group 6

(c)

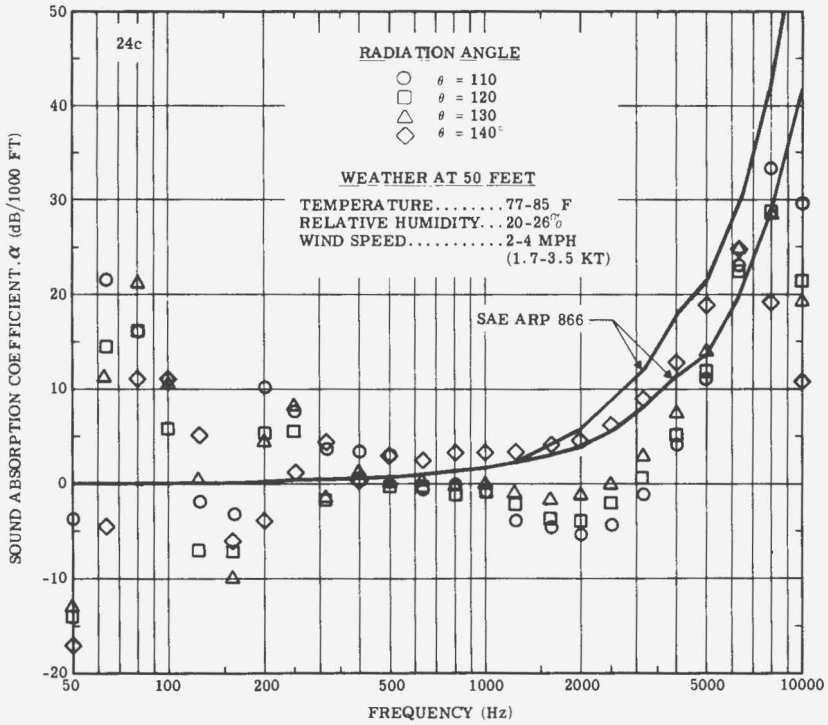

$\beta < 15°$; Z = 100 Feet; X = 500, 1000 Feet

(d)

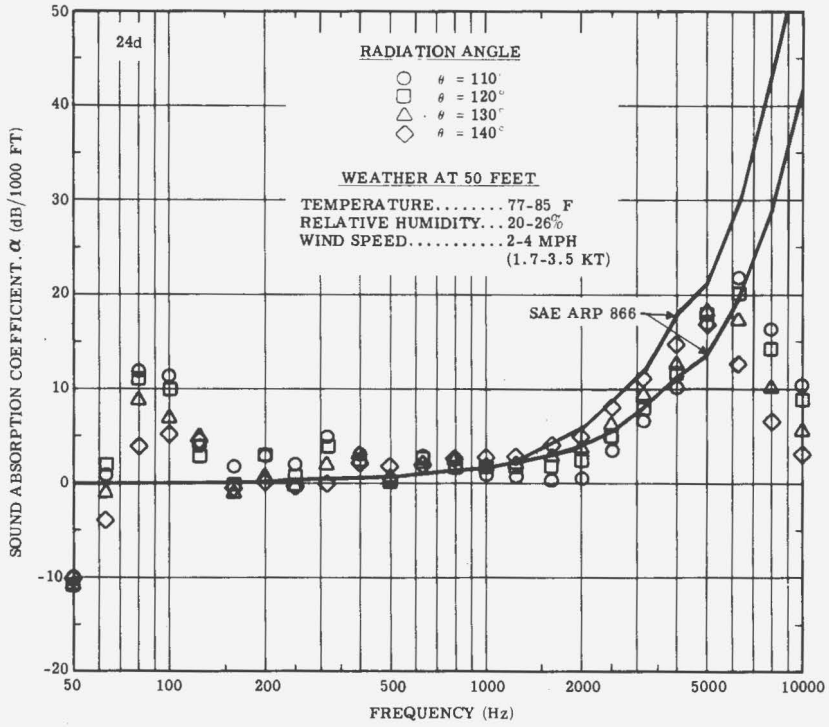

$\beta > 15°$; Z = 100 Feet, X = 500, 1500 Feet

Figure 24. Sound Absorption Coefficients, Test Group 6 (Contd)

(a)

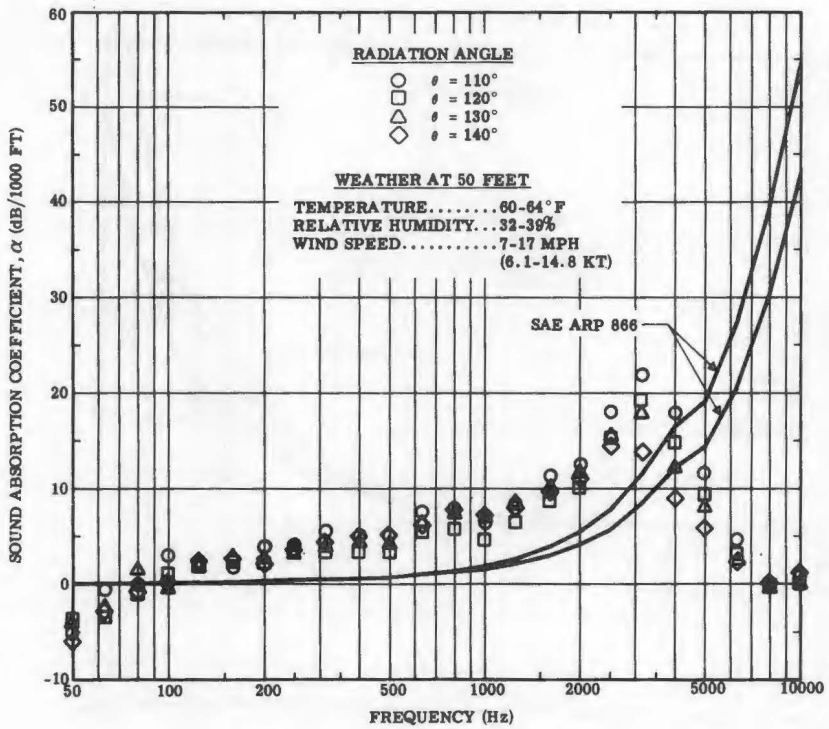

$\beta > 15°$; Z $\geq$ 700 Feet; X = 250, 500, 1000, 1500 Feet

(b)

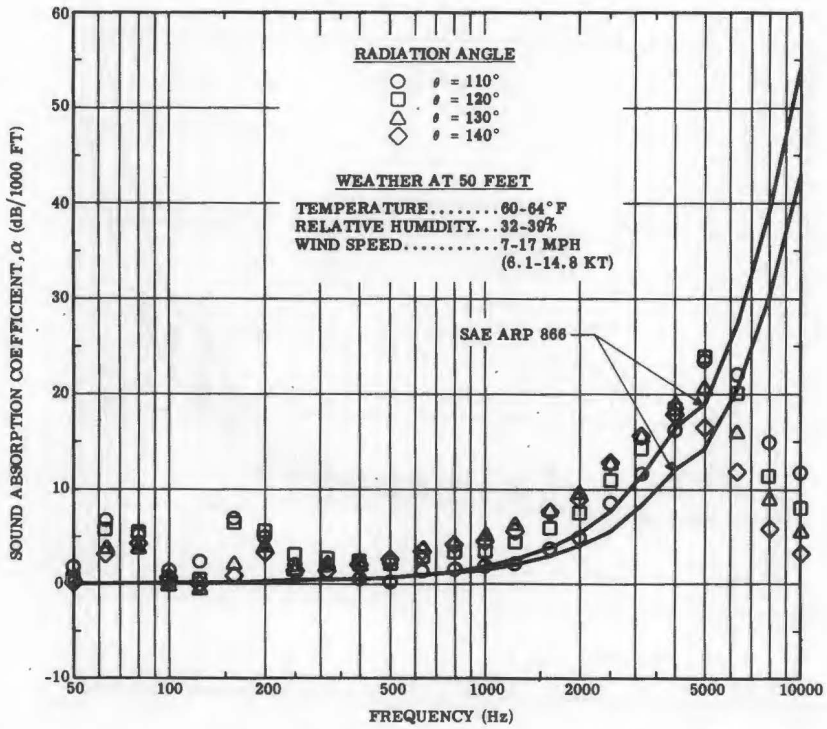

$\beta < 15°$; Z = 100 Feet; X = 250, 500, 1000, 1500 Feet

Figure 25. Sound Absorption Coefficients, Test Group 7

(c)

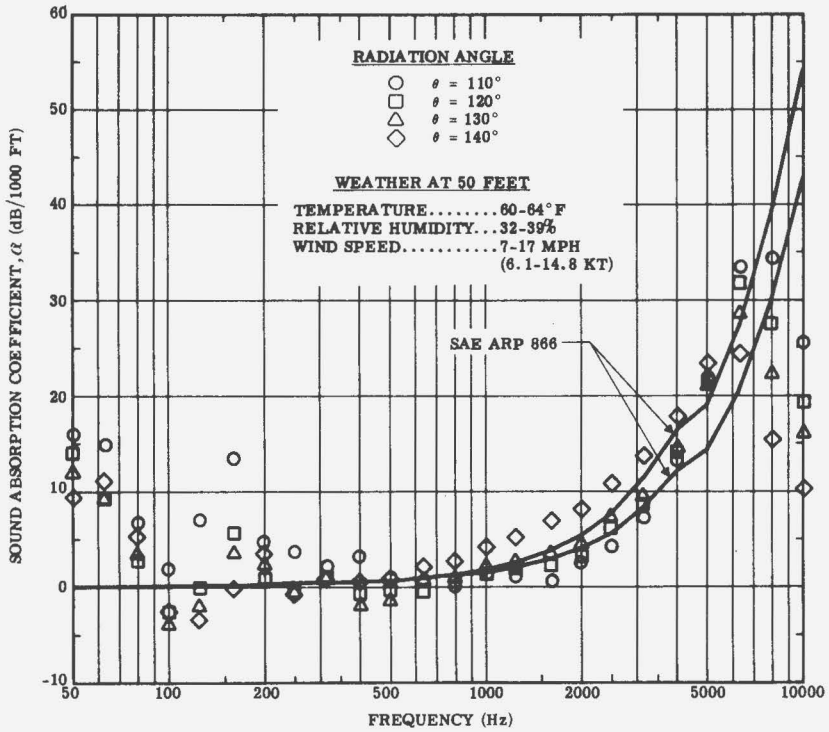

$\beta < 15°$; Z = 100 Feet; X = 500, 1000 Feet

(d)

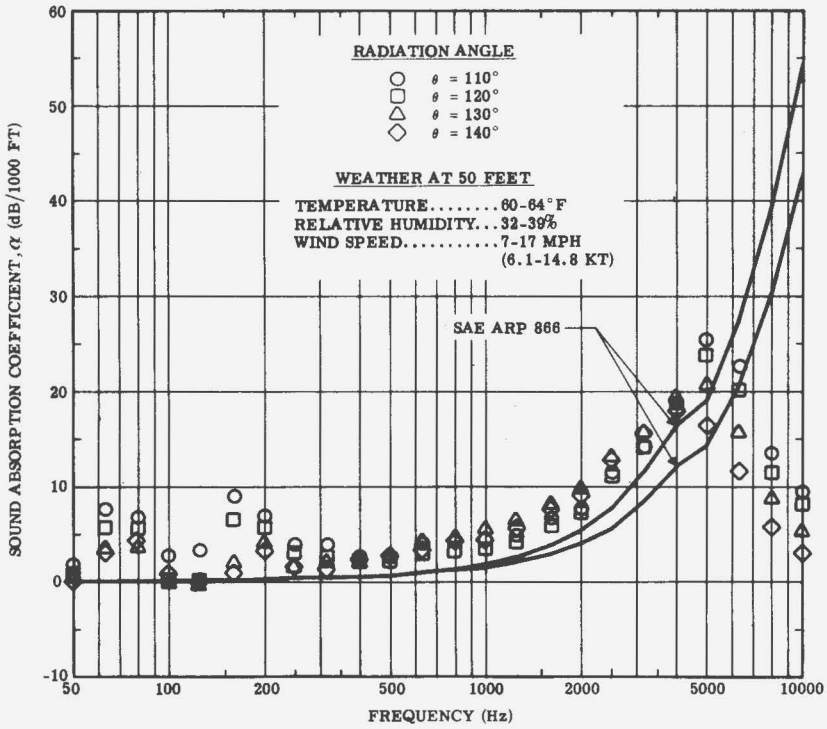

$\beta < 15°$; Z = 100 Feet; X = 500, 1500 Feet

Figure 25. Sound Absorption Coefficients, Test Group 7 (Contd)

(a)

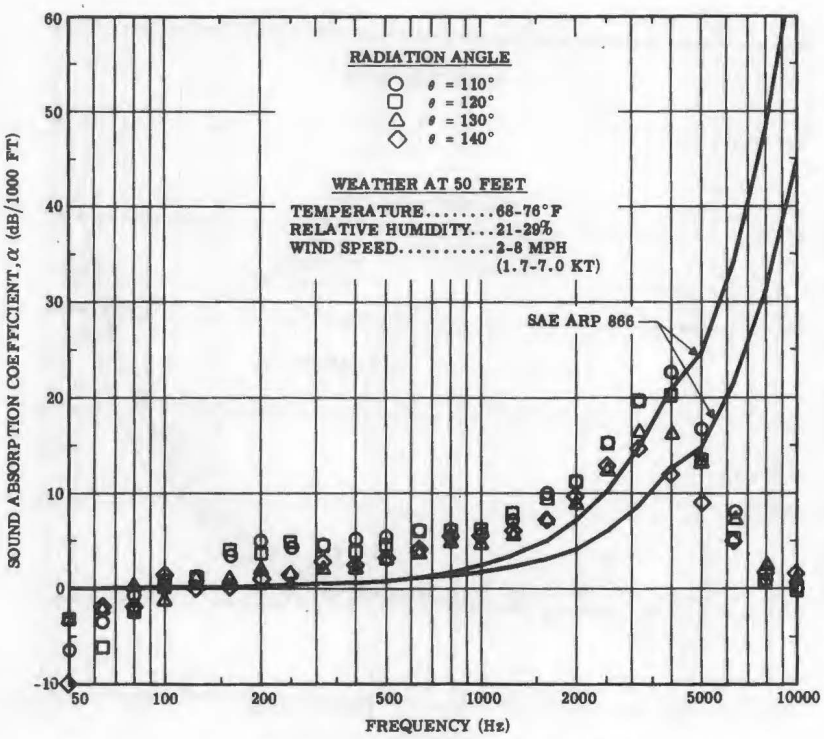

$\beta > 15°$; Z $\geq$ 700 Feet; X = 250, 500, 1000, 1500 Feet

(b)

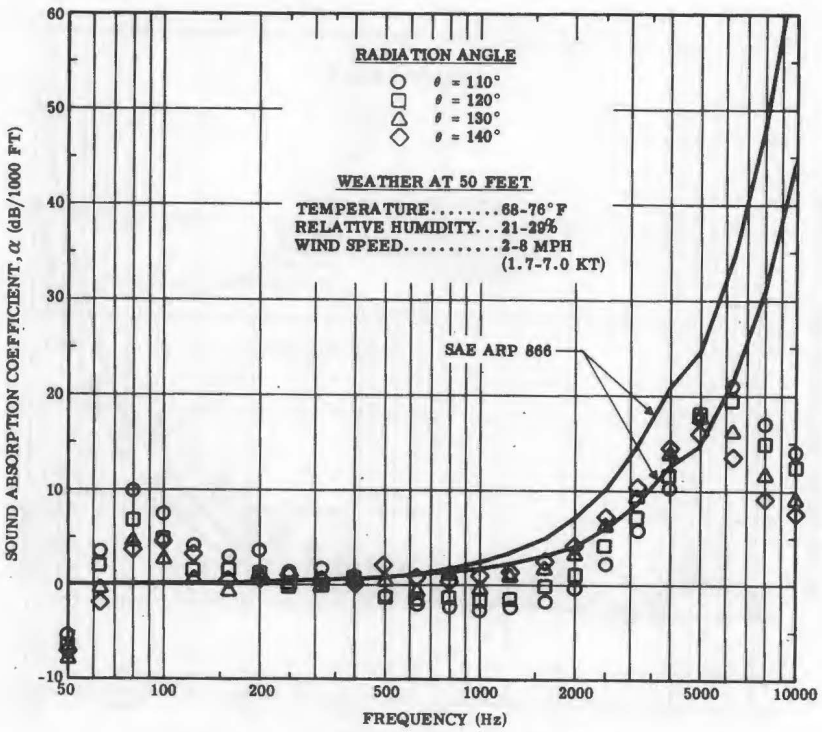

$\beta < 15°$; Z = 100 Feet; X = 250, 500, 1000, 1500 Feet

Figure 26. Sound Absorption Coefficients, Test Group 8

(c)

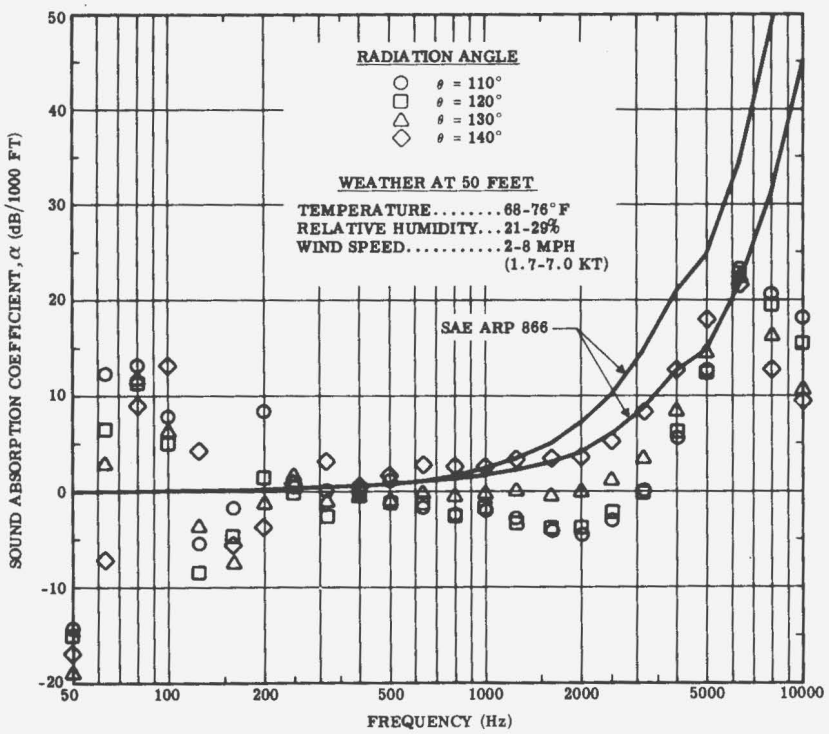

$\beta < 15°$; Z = 100 Feet; X = 500, 1000 Feet

(d)

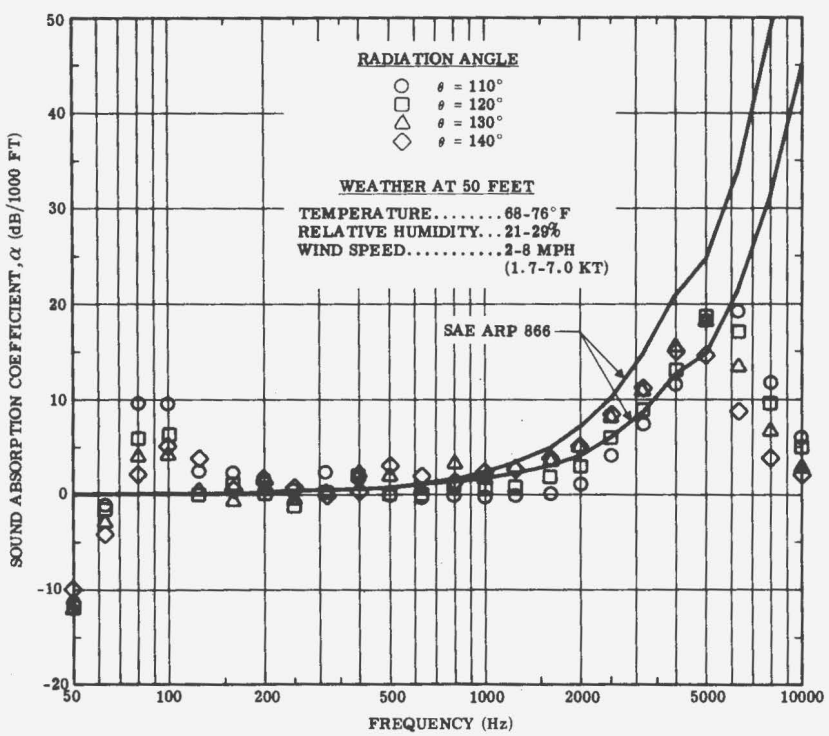

$\beta < 15°$; Z = 100 Feet; X = 500, 1500 Feet

Figure 26. Sound Absorption Coefficients, Test Group 8 (Contd)

(a)

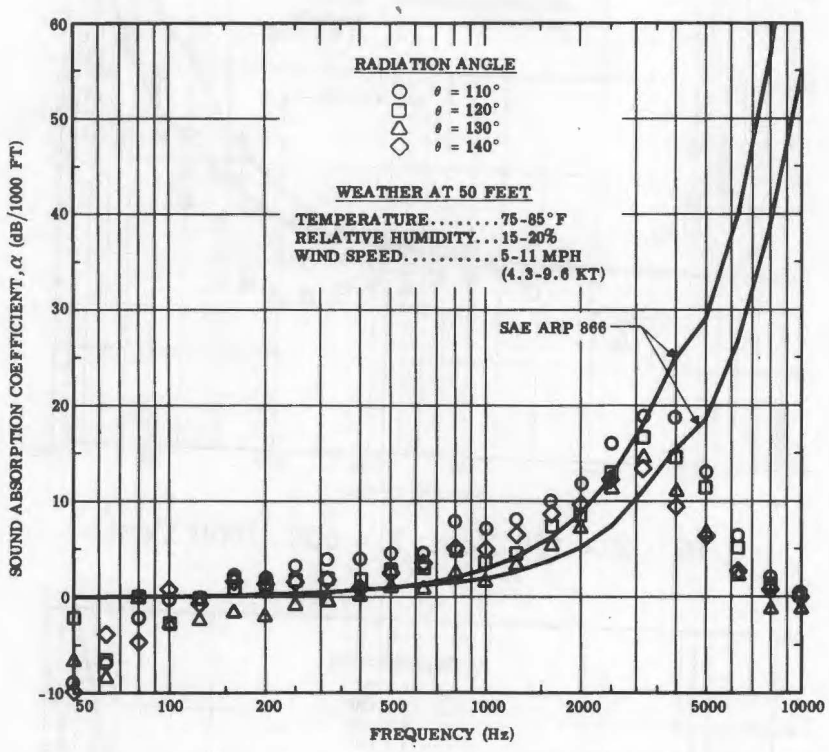

$\beta > 15°$; $Z \geq 700$ Feet; X = 250, 500, 1000, 1500 Feet

Figure 27. Sound Absorption Coefficients, Test Group 9

(a)

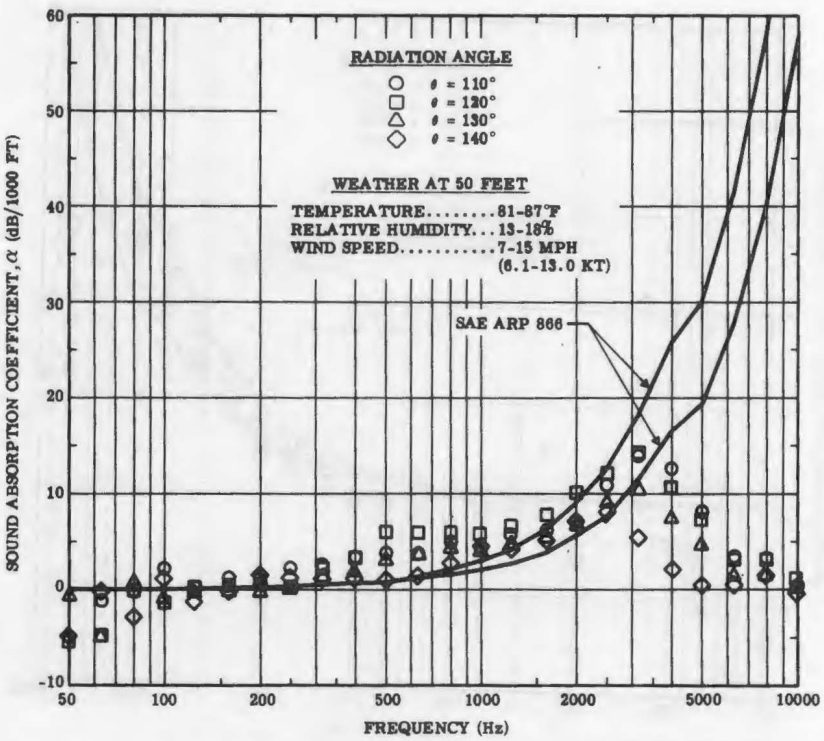

$\beta > 15°$; $Z \geq 700$ Feet; X = 250, 500, 1000, 1500 Feet

(b)

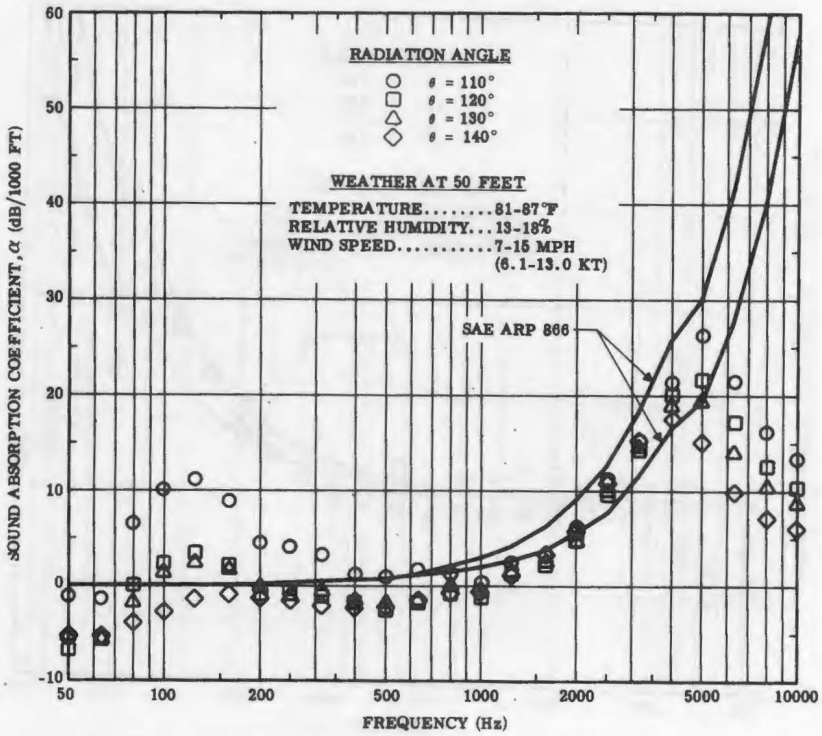

$\beta < 15°$; Z = 100 Feet; X = 250, 500, 1000, 1500 Feet

Figure 28. Sound Absorption Coefficients, Test Group 10

(c)

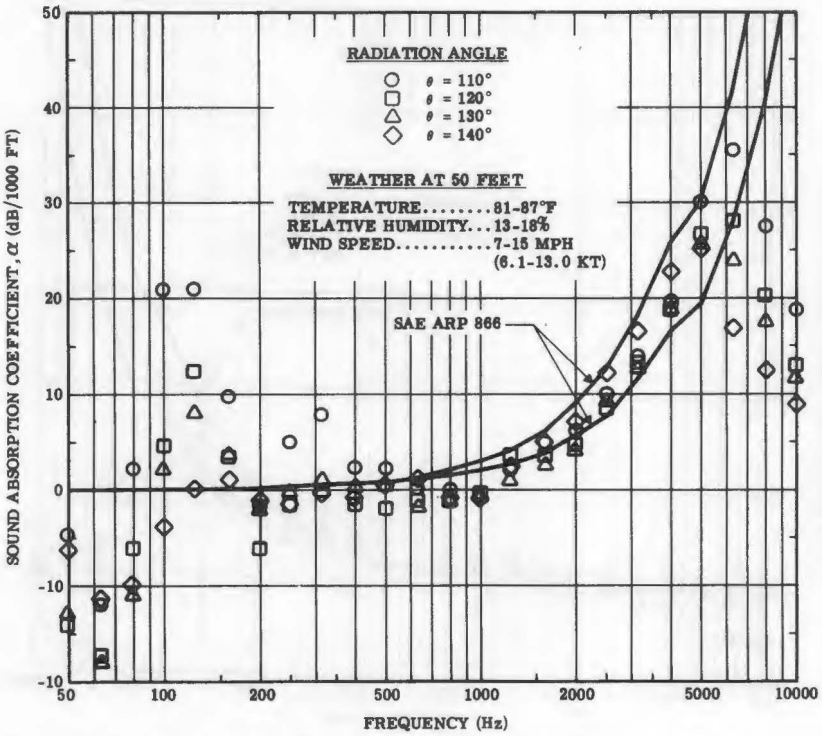

$\beta < 15°$; Z = 100 Feet; X = 500, 1000 Feet

(d)

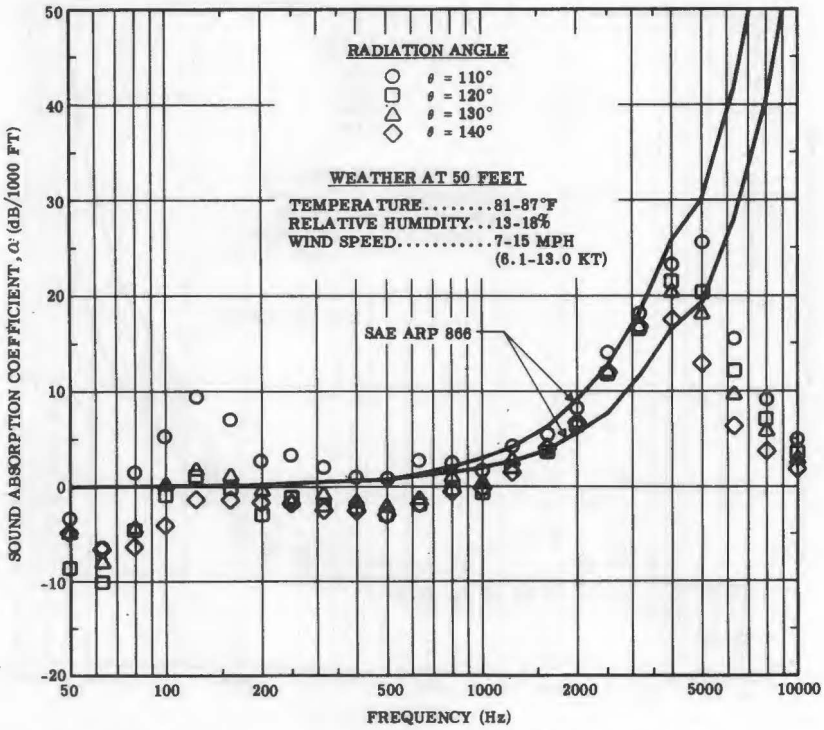

$\beta < 15°$; Z = 100 Feet; X = 500, 1500 Feet

Figure 28. Sound Absorption Coefficients, Test Group 10 (Contd)

CONCLUSIONS

A comparison of experimental absorption coefficients and those calculated from ARP 866 for elevation angles greater than 15 degrees indicate, in general, greater air-to-ground absorption for the test data. For angles of elevation less than 15 degrees, the test data agree with, and occasionally, fall below the calculated band of ARP 866 data.

The test results represent data for some extreme relative humidity conditions. Based on these results, it appears that ARP 866 tends to slightly underestimate the atmospheric absorption for air-to-ground propagation for frequencies below 5000 Hz. The data for frequencies greater than 5000 Hz are inconclusive since these data are subject to error caused by a decreasing signal-to-noise ratio.

REFERENCES

1. Carole S. Tanner, "Measurement and Analysis of Noise from Seventeen Aircraft in Level Flight (Military, Business Jet, and General Aviation Aircraft)," Federal Aviation Administration Report FAA-RD-71-98, November 1971.

2. "Jet Noise Prediction," Society of Automotive Engineers, AIR 876, 10 July 1965.

3. "Standard Values of Absorption as a Function of Temperature and Humidity for Use in Evaluating Aircraft Flyover Noise," Society of Automotive Engineers, ARP 866, April 1970 (Proposed).

Appendix A

FLYBY MEASUREMENT GEOMETRY

PROBLEM:

A plane flies along a horizontal track past a group of microphones layed out along a line perpendicular to the plane track. The plane is assumed to maintain a pitched-up attitude during its pass, but no yaw. The axis of symmetry of the aircraft noise field is assumed to be along the centerline of the airplane at the same pitched-up attitude. Given the height of the plane, the perpendicular distance from the plane's ground track to the microphone, the pitch-up angle, and a directivity angle relative to the plane centerline, what is the corresponding distance along the track of the plane from the point where the specified angle occurs as seen at the microphone and the CPA?

ASSUMPTIONS:

It is assumed that the ground is horizontal, the plane track is horizontal and perpendicular to the line of microphones, and the plane attitude contains no component in the direction of the microphones.

METHOD OF SOLUTION:

A specified directivity angle defines a cone centered on the airplane and tilted upward at the pitch-up angle. The intersection of this conic surface and the ground plane is a curved line at any point along which the required directivity angle will be observed. The curved line is either an elipse, hyperbola, or parabola depending on the values of the parameters. The point along this curve that is the specified horizontal distance in a perpendicular direction from the plane's ground track is the microphone position.

DETAILED SOLUTION:

To get the equation of the cone, choose a coordinate system x, y′, z′ tilted relative to the horizontal such that the origin is centered on the plane and the y′-axis is lined up with the plane's centerline.

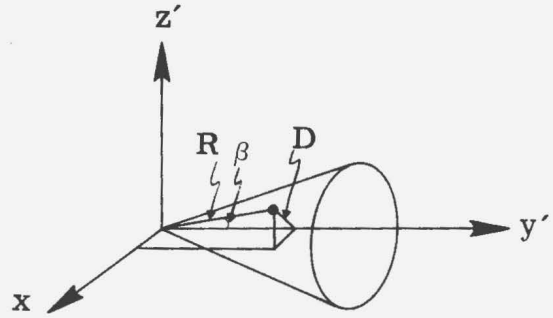

To get the equation of the cone, consider a point on the surface as shown in the figure with coordinates x, y′, z′. The distance R is

$$R = \sqrt{x^2 + y'^2 + z'^2} \tag{1}$$

The line D is perpendicular to the y′ axis with length

$$D = \sqrt{x^2 + z'^2} \tag{2}$$

<u>R</u> and <u>D</u> form a right triangle with an angle

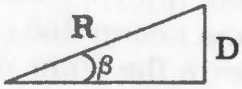

which is the half-angle of the cone. Hence

$$\sin\beta = \frac{D}{R} \tag{3}$$

Putting Equations 1 and 2 into Equation 3, we get the equation of the cone:

$$\sin\beta = \sqrt{\frac{x^2 + y'^2}{x^2 + y'^2 + z'^2}} \tag{4}$$

Squaring, we get after rearrangement

$$x^2(1 - \sin^2\beta) + z'^2(1 - \sin^2\beta) - y'^2\sin^2\beta = 0$$

or

$$\boxed{\cos^2\beta(x^2 + z'^2) - \sin^2\beta(y'^2) = 0} \tag{5}$$

EQUATION OF CONE

as the final equation.

The equation of the cone in a coordinate system, x, y, z where z is vertical and y is parallel to the plane's track is obtained by a standard coordinate rotation by an angle α (the pitch-up angle).

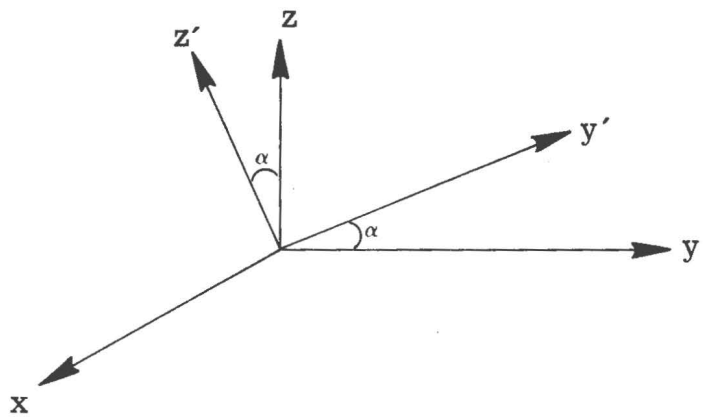

The equations relating the two coordinate systems are

$$\left.\begin{aligned} z' &= z\cos\alpha - y\sin\alpha \\ y' &= z\sin\alpha + y\cos\alpha \\ x &= x \end{aligned}\right\} \tag{6}$$

Expressed in x, y, z coordinates the equation of the cone is

$$\boxed{\cos^2\beta\left[x^2 + (z\cos\alpha - y\sin\alpha)^2\right] - \sin^2\beta\left[z\sin\alpha + y\cos\alpha\right]^2 = 0} \tag{7}$$

EQUATION OF TILTED CONE

where

β = half-angle of cone

α = tilt angle

Now the equation of the ground plane is simply

$$\boxed{z = -H} \tag{8}$$

EQUATION OF GROUND PLANE

where H is the height of the airplane. Remember that the origin of the coordinate system is centered at the airplane.

Simultaneous solution of Equations 7 and 8 yields the equation of the line of intersection of the two surfaces:

$$\boxed{\cos^2\beta\left[x^2 + (-H\cos\alpha - y\sin\alpha)^2\right] - \sin^2\beta(-H\sin\alpha + y\cos\alpha)^2 = 0} \qquad (9)$$

EQUATION OF LINE OF CONSTANT β ON GROUND PLANE

Collecting terms

$$\cos^2\beta\, x^2 + \cos^2\beta\cos^2\alpha\, H^2 + 2\cos^2\beta\cos\alpha\sin\alpha\, Hy$$

$$+ \cos^2\beta\sin^2\alpha\, y^2 - \sin^2\beta\sin^2\alpha\, H^2$$

$$+ 2\sin^2\beta\sin\alpha\cos\alpha\, Hy - \sin^2\beta\cos^2\alpha\, y^2 = 0$$

or

$$\cos^2\beta\, x^2 + (\cos^2\beta\sin^2\alpha - \sin^2\beta\cos^2\alpha)\, y^2$$

$$+ (\cos^2\beta + \sin^2\beta)\sin 2\alpha\, Hy$$

$$+ (\cos^2\beta\cos^2\alpha - \sin^2\beta\sin^2\alpha)\, H^2 = 0$$

Now

$$\sin^2\alpha\cos^2\beta - \sin^2\beta\cos^2\alpha = (\sin\alpha\cos\beta + \cos\alpha\sin\beta)$$

$$\times (\sin\alpha\cos\beta - \cos\alpha\sin\beta)$$

$$= \sin(\alpha + \beta)\sin(\alpha - \beta)$$

$$= \frac{1}{2}\cos 2\beta - \frac{1}{2}\cos 2\alpha$$

$$= \frac{1}{2}(\cos 2\beta - \cos 2\alpha)$$

We get

$$\boxed{(\cos^2\beta)x^2 + \frac{1}{2}(\cos 2\beta - \cos 2\alpha)y^2 + \sin 2\alpha\, H y = -\frac{1}{2}(\cos 2\alpha + \cos 2\beta)H^2} \quad (11)$$

α = angle of attack

β = $\frac{1}{2}$ angle of cone

H = altitude

y = track along centerline, x = distance to side

This can be put into the "normal" form by completing squares:

$$(\cos^2\beta)x^2 + \frac{1}{2}(\cos 2\beta - \cos 2\alpha)y^2 + \sin 2\alpha H y + \frac{\sin^2 2\alpha H^2}{2(\cos 2\beta - \cos 2\alpha)}$$

$$= \left[-\frac{1}{2}(\cos 2\alpha + \cos 2\beta) + \frac{\sin^2 2\alpha}{2(\cos 2\beta - \cos 2\alpha)}\right]H^2$$

or

$$(\cos^2\beta)x^2 + \left[\sqrt{\frac{1}{2}(\cos 2\beta - \cos 2\alpha)}\; y + \frac{\sin 2\alpha}{2\sqrt{\frac{1}{2}(\cos 2\beta - \cos 2\alpha)}} H\right]^2$$

$$= \frac{1}{2}\left[\frac{\sin^2 2\alpha}{(\cos 2\beta - \cos 2\alpha)} - (\cos 2\beta + \cos 2\alpha)\right]H^2$$

or

$$(\cos^2\beta)x^2 - \frac{1}{2}(\cos 2\alpha - \cos 2\beta)\left[y - \frac{\sin 2\alpha\, H}{(\cos 2\alpha - \cos 2\beta)}\right]^2$$

$$= \frac{1}{2}\left[-\frac{\sin^2 2\alpha}{(\cos 2\alpha - \cos 2\beta)} - (\cos 2\beta + \cos 2\alpha)\right]H^2$$

or

$$= -\frac{\sin^2 2\beta}{2(\cos 2\alpha - \cos 2\beta)} H^2$$

or

$$\boxed{\frac{(y-k)^2}{A^2} - \frac{x^2}{B^2} = 1 \qquad \text{EQUATION OF CONIC SECTION}} \tag{12}$$

where

$$A = \frac{\sin 2\beta}{(\cos 2\alpha - \cos 2\beta)} H \tag{13}$$

$$B = \sqrt{\frac{2\sin^2\beta}{(\cos 2\alpha - \cos 2\beta)}}\, H \tag{14}$$

$$k = \frac{\sin 2\alpha}{(\cos 2\alpha - \cos 2\beta)} H \tag{15}$$

The solution of the problem involves solving Equation 12 for y in terms of the microphone distance x, the pitch-up angle α, and the directivity angle β. We get

$$y = k \pm \sqrt{A^2\left(1 + \frac{x^2}{B^2}\right)} \tag{16}$$

where A, B, and k are given above.

Unfortunately, the solution in the form given by Equation 16 is inconvenient for certain values of β because A, B, and k go to infinity in such a way that y remains finite. Also, B^2 and k can take on both positive and negative values. This obscures which solution of Equation 16 to choose. To see this, consider the quantity

$$u = \cos 2\alpha - \cos 2\beta$$

This can be rewritten in the form

$$u = 2\sin(\beta + \alpha)\sin(\beta - \alpha) \tag{17}$$

For the range of values $0° < \beta < 180°$, it is easy to see that u is zero when $\beta + \alpha = 180°$ or when $\beta - \alpha = 0°$. Similarly, when $\beta > 180 - \alpha$ or $\beta < \alpha$ then u will be negative. Since u is the <u>denominator</u> of A, B^2, and k, it is evident that these quantities can go infinite or negative. To see that y remains finite, consider the case $u \to 0$. Then $A \to \infty$, $B^2 \to \infty$, $k \to \infty$. In Equation 16, we have

$$\frac{x^2}{B^2} \ll 1$$

in the limit so that Equation 16 reduces to

$$\begin{aligned} y &= k \pm \sqrt{A^2} \\ &= k \pm A \\ &= H\left[\frac{\sin 2\beta \pm \sin 2\alpha}{u}\right] \end{aligned} \tag{18}$$

If we take the minus sign, then using Equation 17

$$y_- = H\,\frac{2\cos(\beta+\alpha)\sin(\beta-\alpha)}{2\sin(\beta+\alpha)\sin(\beta-\alpha)} = H\cot(\beta+\alpha) \tag{19}$$

Taking the plus sign gives

$$y_+ = H\,\frac{2\sin(\beta+\alpha)\cos(\beta-\alpha)}{2\sin(\beta+\alpha)\sin(\beta-\alpha)} = H\cot(\beta-\alpha) \tag{20}$$

Now if $u \to 0$ because $(\beta - \alpha) \to 0$, then $y_+ \to \infty$ but the other solution y_- remains finite. Similarly, if $u \to 0$ because $(\beta + \alpha) \to 0$, then $y_- \to \infty$ but y_+ remains finite. In this discussion, α has been implicitly assumed to be positive. If α were negative, then trouble would occur when $(\beta - \alpha) = 180°$ or $(\beta + \alpha) = 0°$ but the same results would apply.

To recast Equation 16 in a useful form, we first make the assumption that $\alpha > 0$ and that calculations are restricted to the range

$$\left.\begin{aligned} 0 < \beta < 180 \\ (\beta - \alpha) > 0 \end{aligned}\right\} \tag{21}$$

This means that the only limit problem occurs when $\beta + \alpha = 180°$. For this case, the plus solution given by Equation 20 is the correct limiting form; namely,

$$y = k + A = H \cot(\beta - \alpha) \tag{22}$$
$$\beta + \alpha \rightarrow 180$$

This suggests that we recast Equation 16 in the form

$$y = (k + A) + [\text{EXTRA TERM}] \tag{23}$$

and replace k + A by the equivalent term Equation 22 so that we do not have to subtract two infinite terms as is necessary in Equation 16.

Now Equation 16 can be written as

$$y = k + A - \left[A \mp \sqrt{A^2\left(1 + \frac{x^2}{B^2}\right)}\right]$$

$$= H \cot(\beta - \alpha) - \left[A \mp \sqrt{A^2\left(1 + \frac{x^2}{B^2}\right)}\right] \tag{24}$$

The term in the square brackets can be simplified using the relation

$$(p^2 - q^2) = (p + q)(p - q)$$

or

$$(p \mp q) = \frac{(p^2 - q^2)}{(p \pm q)} \tag{25}$$

We get

$$y = H \cot(\beta - \alpha) - \frac{\left[A^2 - A^2\left(1 + \frac{x^2}{B^2}\right)\right]}{\left[A \pm \sqrt{A^2\left(1 + \frac{x^2}{B^2}\right)}\right]}$$

or

$$y = H\cot(\beta - \alpha) + \frac{A^2 \dfrac{x^2}{B^2}}{A\left[1 \pm \sqrt{1 + \dfrac{x^2}{B^2}}\right]} \tag{26}$$

Now from Equations 13 and 14

$$\frac{A}{B^2} = \frac{\dfrac{H \sin 2\beta}{u}}{\dfrac{2 H^2 \sin^2\beta}{u}} = \frac{2 \sin\beta \cos\beta}{2 H \sin^2\beta} = \frac{\cot\beta}{H} \tag{27}$$

$$\frac{1}{B^2} = \frac{u}{2 H^2 \sin^2\beta} \tag{28}$$

Using these in Equation 26 and simplifying, we get

$$y = H\cot(\beta - \alpha) + \frac{\dfrac{x^2 \cot\beta}{H}}{\left[1 \pm \sqrt{1 + \dfrac{u}{2\sin^2\beta}\dfrac{x^2}{H^2}}\right]} \tag{29}$$

If the minus sign is chosen, the solution blows up when $u \to 0$ (i.e., $\beta + \alpha \to 180°$). Therefore, we choose the plus sign solution as our final form

$$\boxed{y = H\left[\cot(\beta - \alpha) + \frac{(x/H)^2 \cot\beta}{1 + \sqrt{1 + \dfrac{u\,(x/H)^2}{2\sin^2\beta}}}\right]} \tag{30}$$

FINAL SOLUTION

where

$$u = \cos 2\alpha - \cos 2\beta$$

$$0 < \beta < 180$$

$$\beta > \alpha > 0$$

$$\left[1 + \frac{u\,(x/H)^2}{2\sin^2\beta}\right] > 0$$

GEOMETRIC SIGNIFICANCE:

The geometric significance of $u \to 0$ or equivalently $\beta + \alpha \to 180$ is shown in the figure below. We see the $\beta + \alpha \to 180$ corresponds to the upper surface of the cone becoming horizontal. For $\beta + \alpha > 180$ (which gives $u < 0$), the intersection of the cone with the ground is an elipse – which may give two points at the required perpendicular distance x. This is shown in the following sketch.

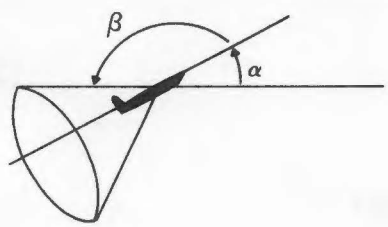

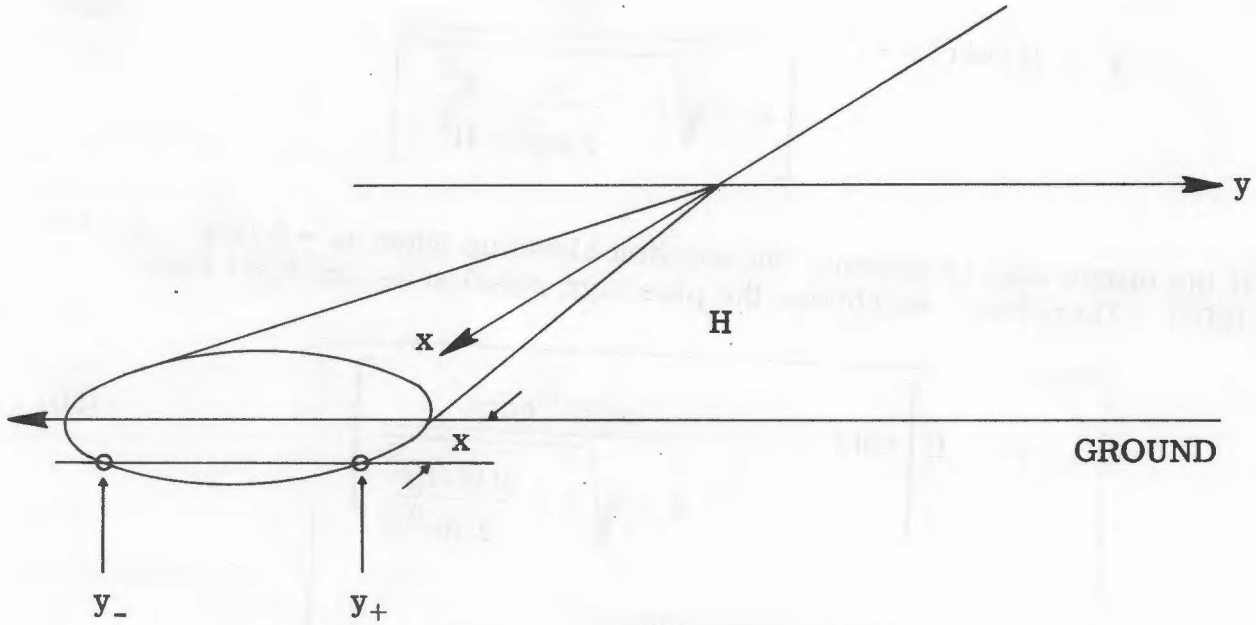

The point y_+ is obtained by taking the plus sign in Equation 29; the point y_- is obtained by taking the minus sign. Since the closest distance normally is of interest, the plus solution (Equation 3) is used. For certain values of the parameters, the elipse is so narrow that no part of it is a distance $\underline{x}$ away. This occurs when the radicand of Equation 30 goes negative.

$$1 + \frac{u\,(x/H)^2}{2\sin^2\beta} < 0$$

CONDITION FOR NO SOLUTION

22782